On the Role of Rossby Wave Breaking in the Quasi-Biennial Modulation of the Stratospheric Polar Vortex during Boreal Winter

Hua Lu[1,a], Matthew H. Hitchman[b], Lesley J. Gray[c], James A. Anstey[d] and Scott M. Osprey[c]

[1]Corresponding author Email: hlu@bas.ac.uk

[a] *British Antarctic Survey, High Cross, Madingley Road, Cambridge CB3 0ET, United Kingdom. (hlu@bas.ac.uk)*

[b] *Department of Atmospheric and Oceanic Sciences, University of Wisconsin – Madison, 1225 West Dayton Street Madison, WI 53706, USA (matt@aos.wisc.edu)*

[c] *NCAS-Climate, Department of Atmospheric Physics, Oxford University, Clarendon Laboratory, Parks Road, Oxford, OX1 3PU, United Kingdom (gray@atm.ox.ac.uk; Scott.Osprey@physics.ox.ac.uk)*

[d] *Canadian Centre for Climate Modelling and Analysis, Environment and Climate Change Canada, Victoria, British Columbia, Canada (james.anstey@canada.ca)*

This article has been accepted for publication and undergone full peer review but has not been through the copyediting, typesetting, pagination and proofreading process which may lead to differences between this version and the Version of Record. Please cite this article as doi: 10.1002/qj.3775.

Abstract: The boreal-winter stratospheric polar vortex is more disturbed when the quasi-biennial oscillation (QBO) in the lower stratosphere is in its easterly phase (eQBO), and more stable during the westerly phase (wQBO). This so-called "Holton-Tan effect" (HTE) is known to involve Rossby waves (RWs) but the details remain obscure.

This tropical-extratropical connection is re-examined in an attempt to explain its intra-seasonal variation and its relation to Rossby wave breaking (RWB). Reanalyses in isentropic coordinates from the National Center for Environmental Prediction Climate Forecast System for the 1979 – 2017 period are used to evaluate the relevant features of RWB in the context of waveguide, wave mean-flow interaction, and the QBO-induced meridional circulation. During eQBO, the net extratropical wave forcing is enhanced in early winter with ~25% increase in upward propagating PRWs of zonal wavenumber 1 (wave-1). RWB is also enhanced in the lower stratosphere, characterized by convergent anomalies in the subtropics and at high-latitudes and strengthened waveguide in between at 20-40°N, 350-650 K. In late winter, RWB leads to finite amplitude growth, which hinders upward propagating PRWs of zonal wavenumber 2 and 3 (wave-2-3). During wQBO, RWB in association with wave-2-3 is enhanced in the upper stratosphere. Wave absorption/mixing in the surf zone reinforces a stable polar vortex in early to middle winter. A poleward confinement of extratropical waveguide in the upper stratosphere forces RWB to extend downward around January. A strengthening of upward propagating wave-2-3 follows and the polar-vortex response switches from reinforcement to disturbance around February, thus a sign reversal of the HTE in late winter.

Keywords: Quasi-biennial oscillation; stratospheric polar vortex; Rossby wave breaking; Holton-Tan effect.

1. Introduction

The polar vortex is the westerly circumpolar jet in the winter stratosphere, which owes its existence to the equator-to-pole temperature gradient (Andrews *et al*., 1987). The vortex varies in strength in response to upward propagation of planetary-scale Rossby waves (PRWs) emanating from the troposphere (Scherhag, 1952; Matsuno, 1971). Disturbances due to PRWs can result in extreme vortex events, i.e. stratospheric sudden warmings (SSWs), which are known to affect surface climate up to a few months (Baldwin and Dunkerton, 1999; Kidston *et al*., 2015). It is important to capture stratosphere variability and the associated downward influences because it has been shown that incorporating stratospheric processes into forecast models can lead to improved weather prediction, especially on sub-seasonal to seasonal time-scales (e.g. Marshall and Scaife, 2009). The mechanism(s) are however not fully understood because the propagation of PRWs and their subsequent breaking and absorption by the background mean flow are influenced by other factors (McIntyre, 1982; Kidston *et al*., 2015).

The factors that are known to influence PRWs include the El Niño/Southern Oscillation (e.g. Domeisen *et al*., 2019), major volcanic eruptions (e.g. Kodera, 1994; Robock, 2000), Eurasian snow cover extent or Artic sea-ice (Cohen and Entekhabi, 1999; Nakamura *et al*., 2016; Labe *et al*., 2019), solar ultraviolet irradiance (e.g. Gray *et al*., 2010; Lu *et al*., 2017) and the quasi-biennial oscillation (QBO) (Baldwin *et al*., 2001; Gray *et al*., 2018). The QBO is a tropical phenomenon characterized by alternating descending easterly and westerly winds with a period ranging from 24 to 32 months (Baldwin *et al*., 2001; Schenzinger *et al*., 2017). Holton and Tan (1980) found that the boreal-winter stratospheric polar vortex was more disturbed when the QBO in the lower stratosphere was in its easterly phase but remains stable when the QBO was in its westerly phase.

This so-called "Holton-Tan effect" (HTE) has been linked to the occurrence and/or timing of SSWs, with SSWs occurring more frequently during the easterly QBO winters than westerly QBO winters (Labitzke, 1982; Dunkerton and Baldwin, 1991; Gray *et al*., 2004). The strength of the HTE also varies on multi-decadal time-scales and is further affected by the 11-year solar cycle (Gray *et al*., 2004; Lu *et al*., 2008; 2014). Considerable progress has been made in reproducing the QBO itself in more comprehensive climate models recently via improved parametrization of small-scale waves with increased vertical resolution (Geller *et al*., 2016, Butchart *et al*., 2018). But replicating the HTE with the observed strength remains a challenge (Garfinkel *et al.*, 2018; Zhang *et al*., 2019).

The classic mechanism involves changes in the winter stratospheric waveguide in response to a latitudinal shift of the zero-wind line (Holton and Tan, 1980). When the QBO is in its easterly phase, the zero-wind line is shifted into the subtropical winter hemisphere. PRWs are thus confined more towards the extratropical winter stratosphere and the vortex weakens in response to this enhanced wave forcing. Conversely, when the QBO is in its westerly phase, the zero-wind line is in the summer hemisphere. A wider than normal waveguide in the winter hemisphere results in a less disturbed polar vortex. Studies aimed at verifying this mechanism have so far been inconclusive (see Anstey and Shepherd, 2014 for a review). For instance, the refractive index for stationary PRWs has been found to increase in the subtropics and at high latitudes but reduces in the mid-latitudes where the polar-vortex westerlies maximize when the QBO is in its easterly phase (Lu *et al.*, 2014; Zhang *et al*., 2019). QBO modulation of wave mean-flow interaction differs distinctively from the lower and upper stratospheres (Yamashita *et al.*, 2011; Garfinkel *et al*., 2012). Furthermore, the upward Eliassen-Palm (EP) fluxes F_z in the mid-latitude lower stratosphere was found to differ comparatively little between the two QBO phases during mid-winter season (e.g.

Baldwin and Dunkerton, 1991; Calvo *et al.*, 2007). Instead, the QBO anomaly in F_z in the lower stratosphere has been found to reverse in sign between early and late winter (e.g. Hitchman and Huesmann, 2009 (HH09); Naoe and Shibata, 2010; White *et al*., 2016). F_z of zonal wavenumber 1 was enhanced in early winter when the QBO was in its easterly phase, but an enhancement of zonal wavenumber 2 was detected in late winter in assocaition with the westerly QBO (Hu and Tung, 2002; Ruzmaikin *et al*., 2005). These responses cannot be fully explained by the classic mechanism. It has been suggested that changes in the zero-wind line location may also alter extratropical wave forcing via poleward wave reflection (Tung, 1979; Holton and Tan, 1982). Watson and Gray (2014) studied this effect using a climate model and found anomalous poleward wave propagation from the height region where the QBO zero-wind line is located in the winter hemisphere. However, such a response could only be observed during the first few days of the model integration.

Zonal winds in the equatorial upper stratosphere in determining polar vortex variability have also been reported (Gray *et al*., 2003; Pascoe *et al*., 2006). When easterly wind anomalies were imposed in the equatorial upper stratosphere, the disruption to the polar vortex tends to occur earlier than average (Gray *et al*., 2003). Pascoe *et al.* (2006) later found that the main impact of the equatorial upper stratospheric wind anomaly was on the timing of SSWs; SSWs were delayed when the zonal winds in the equatorial upper stratosphere were strong westerlies while SSWs occurs earlier when easterly anomalies are found in the equatorial or subtropical upper stratosphere. The importance of QBO-induced changes in EP-flux convergence in the middle to upper stratosphere have also been reported by other studies (e.g. Calvo *et al.,* 2007; Garfinkel *et al*., 2012; Lu *et al*., 2014).

Studies have also suggested that the QBO-induced mean meridional circulation (QBO-MMC) plays an important role in the HTE (Ruzmaikin *et al*., 2005; Gray *et al*., 2004; Garfinkel *et al*., 2012). Garfinkel *et al*. (2012) performed model simulations by imposing the QBO at the equator. They found that synoptic-scale Rossby waves (SRWs) are enhanced in the subtropical lower stratosphere during easterly-QBO winters. Breaking of SRWs in the vicinity of the subtropical westerly jet (SWJ) results in a poleward expansion of the region with positive meridional gradients of potential vorticity (PV) (Garfinkel and Hartmann, 2011b). More PRWs are able to enter the extratropical stratosphere as a result. The increase of SRWs in the subtropical lower stratosphere during easterly QBO winters was attributed to the QBO-MMC (Garfinkel and Hartmann, 2011b; Garfinkel *et al*., 2012). However, using a reanalysis data set, White *et al.* (2016) found that the increase in SRWs in the subtropical lower stratosphere was only statistically significant in late winter when the HTE is weak. Furthermore, Gray *et al.* (2003) and Naito and Yoden (2006) imposed easterly wind anomalies to encompass the entire tropics between the lower stratosphere and the lower mesosphere, effectively remove the QBO-MMC. A "HTE-like" response was also detected.

PRWs propagate upward into the winter stratosphere due to strong vertical wind shear in the lower stratosphere. Those waves are then refracted equatorward where they encounter the zero-wind line that separates the westerly winds in the winter hemisphere from the tropical easterlies. Changes in wave absorption or reflection near the zero-wind line would alter the net wave forcing on the polar vortex (Tung, 1979; Killworth and McIntyre, 1985). In the context of the HTE, we would expect QBO-altered zero-wind line to affect meridional wave transport via Rossby wave breaking (RWB), which is a common phenomenon in the winter stratosphere. During a RWB event,

filaments of air are stripped from the polar vortex edge and mixed into the surrounding region (McIntyre and Palmer, 1983; 1984; Leovy *et al*., 1985). Wave disturbances can also span from the tropical zero-wind line to the polar vortex, providing a direct means of coupling between low and high latitudes (O'Sullivan and Salby, 1990).

An individual RWB event is rarely responsible for an immediate break down of the polar vortex, either minor or major SSWs (McIntyre, 1982). Recurrent RWB events reshape the geometry of the stratospheric waveguide and lead to the formation of the surf zone. When the upward propagating waves are of relatively small amplitude, RWB acts to sharpen PV gradients along the vortex edge while irreversible mixing takes place on the equatorward flank of the polar vortex. In the early stage of the development, the region with sharpened PV gradients makes the vortex resistant to further wave disturbances, thus maintaining a stable vortex (Polvani and Saravanan, 2000; Scott and Dritschel, 2005). A sudden, rapid intrusion of low-PV-air into the polar region can take place if the surf zone expands continuously poleward as RWB builds up cumulatively (Albers and Birner, 2014). RWB initialized at upper levels may also gradually extend downward into lower levels to destroy the polar vortex completely (Waugh and Dritschel, 1999; Polvani and Saravanan, 2000). As such, RWB is thought to 'pre-condition' the polar vortex, making it more susceptible to SSWs at a later stage (Limpasuvan *et al*., 2004; Albers and Birner, 2014). These characteristics make RWB differing from the linear theory that accounts for direct wave absorption at the polar vortex edge (Matsuno, 1971).

A large number of studies have been carried out to characterize RWB and its climatology (e.g. Hitchman and Huesmann, 2007; Abatzoglou and Magnusdottir, 2007). For instance, it is found that stratospheric RWB can be broadly classified into upper-level events where PRWs propagate along

the polar vortex edge and break in the upper stratosphere and lower-level events where RWB is confined to the lower stratosphere (Abatzoglou and Magnusdottir, 2007). The upper-level RWB occurs more often in early winter while the lower-level RWB dominates in middle winter. Only a limited number of studies have been devoted to examine the role of RWB in the HTE and its seasonal variation. HH09 calculated the statistics of RWB based on ERA-40 reanalysis data from ECMWF (European Centre for Medium-range Weather Forecasts) over the 1979–2002 period. They found that during December to February, meridional PV gradients in the subtropical lower stratosphere were enhanced during easterly QBO winters while the frequency of RWB was reduced in the same region but opposite anomalies in the upper levels. These results were later confirmed by White *et al.* (2015; 2016) who have found that the QBO-related waveguide and RWB anomalies extended from the subtropics into high latitudes. However, the analyses of White *et al.* (2015; 2016) were confined to the height region between 350 K and 850 K (~100-10 hPa). RWB in the upper stratosphere and its role in the HTE were left unexamined.

The aim of this paper is to provide a more complete picture of the HTE with an improved description of RWB that encompasses the entire stratosphere. A set of diagnostics are performed to examine QBO-related changes in RWB with a special attention paid to its cumulative effect on the polar vortex. The relative importance of RWB is evaluated in the context of extratropical waveguide, wave forcing on the polar vortex, and the QBO-MMC. Contributions from PRWs and SRWs are separately assessed, which allows us to better compare the effect of RWB to wave absorption near the polar vortex edge. A new mechanism is then proposed to explain the observed intra-seasonal variation of the HTE, especially its late winter weakening and/or sign reversal.

2. Data and Methods

2.1. Diagnostics

Ertel's PV in isentropic coordinates provides useful information on the structure and evolution of winter stratospheric dynamics (Hoskins *et al*., 1985). It is given by

$$P = \xi / \sigma \tag{1}$$

where σ is the isentropic density, $\xi = f - \frac{(u\cos\phi)_\phi}{a\cos\phi} + \frac{v_\lambda}{a\cos\phi}$ is the vertical component of absolute isentropic vorticity, f the Coriolis parameter. a the Earth's radius, u, v the zonal and meridional velocities, ϕ latitude, and λ the longitude. PRWs preferentially propagate towards the region where the zonally averaged meridional PV gradient $\overline{P}_\phi$ is large. $\overline{P}_\phi$ is thus used here as a diagnostic for the stratospheric waveguide.

RWB is diagnosed by overturning contours of PV on isentropic surfaces, which is related to momentum deposition of PRWs via RWB (McIntyre and Palmer, 1983; 1984; HH09). Following HH09, RWB frequency is estimated by counting the number of days in which the meridional gradient of Ertel's PV ($\overline{P}_\phi$) becomes negative at each grid point during a pre-selected month or season. The zonal-mean is then taken of this grid-point metric. This zonal-mean metric is denoted as $\overline{\gamma}$ hereinafter and has the units of days per month or season. $\overline{\gamma}$ allows us to examine the extent to which the QBO modulates RWB in terms of relative frequency, location and timing in a statistically averaged sense. $\overline{\gamma}$ does not provide a detailed accounting of the individual events including the size, strength, or duration. This is justified for our purpose as our aim is to compare the relative importance of RWB events between the two QBO phases.

Analyses of $\overline{P}_{\phi}$ and $\overline{\gamma}$ are supplemented by additional diagnostics including the Eliassen-Palm (EP) fluxes and divergence, and down-gradient eddy PV fluxes. Following Andrews *et al.* (1987), the meridional and vertical components of the EP flux in isentropic coordinates are estimated by

$$\begin{aligned} \tilde{F}^{(\phi)} &= -a\cos\phi\overline{(\sigma v)'u'} \\ \tilde{F}^{(\theta)} &= g^{-1}\overline{p'\Psi'_{\lambda}} - a\cos\phi\overline{(\sigma Q)'u'} \end{aligned} \tag{2}$$

where θ is potential temperature, g the gravitational acceleration constant, p pressure, Ψ the Montgomery stream-function, and Q the diabatic heating rate. Overbars denotes zonal averaging on an isentropic surface, subscripts denote derivatives with respect to the given variable, and primes denote departures from the zonal-mean.

The EP-flux divergence $(a\cos\phi)^{-1}\tilde{\nabla}\cdot\tilde{\mathbf{F}} = (a\cos\phi)^{-2}\dfrac{\partial}{\partial\phi}\left(\tilde{F}^{(\phi)}\cos\phi\right) + (a\cos\phi)^{-1}\dfrac{\partial\tilde{F}^{(\theta)}}{\partial\theta}$ is commonly used to diagnose wave forcing on the mean flow. An alternative form of wave forcing in isentropic coordinates is expressed as the density-weighted eddy PV flux on isentropic surfaces (Tung 1986; Andrew *et al*., 1987):

$$\Pi = \overline{\sigma}\overline{\hat{v}\hat{P}}^{*} \tag{3}$$

where the overbar with an asterisk denotes the quantity is a density weighted zonal mean, i.e. $\overline{v}^{*} = \overline{\sigma v}/\overline{\sigma}$ and a caret denotes the departure from the density-weighted zonal average, i.e. $\hat{v} = v - \overline{v}^{*}$. Similar to the EP flux divergence, Π represents the wave forcing per unit of mass on the mean flow and has the units of m s^{-1} day^{-1}. Negative values of Π indicate wave convergence as disturbances of PRWs act to slow down the background westerlies. In this study, $\tilde{F}^{(\phi)}$, $\tilde{F}^{(\theta)}$ and Π

are used together to assess PRW propgation and wave driving. The meridional component of the EP-flux divergence $\Pi_\phi = (a\cos\phi)^{-2}\frac{\partial}{\partial\phi}\left(\tilde{F}^{(\phi)}\cos\phi\right)$ is used as an additional measure of RWB, e.g. large negative values in the stratospheric surf zone together with large positive values at high latitudes indicate enhanced RWB. These quantities are further separated into contributions from planetary waves of zonal wavenumber 1, 2-3 and synoptic-scale Rossby waves (SRWs) where zonal wavenumbers 5-10 are included. Contribution from wave-4 is found to be negligible thus excluded from the analysis.

Meridional transfer of wave activity between the polar vortex edge and the subtropics during RWB events induces changes in enstrophy, i.e. $\overline{P'^2}/2$ (McIntyre and Palmer, 1983). Away from the zero-wind line where the linear wave thoery may break down, the meridional exchange of enstrophy is largely determined by down-gradient eddy PV fluxes (Schoeberl and Smith, 1986; White *et al*., 2015):

$$\Gamma = \overline{P}_\phi \overline{\hat{v}\hat{P}}^* \Big/ a \qquad (4)$$

which is effectively the product of the wave forcing Π and meridional PV gradient $\overline{P}_\phi$. Given that $\overline{P}_\phi$ is generally positive and $\overline{\hat{v}\hat{P}}^*$ is largely negative in the winter stratosphere, Γ must be predominantly negative. Climatologically, we expect down-gradient transfer of PV fluxes to be most strong near the polar vortex edge because RWB acts to "strip off" high-PV airs from the polar vortex edge and "flux out" them sideways (McIntyre and Palmer, 1983; Schoeberl and Smith, 1986). Thus, large negative values of Γ should peak along the flanks of the polar vortex. Γ is used here to examine QBO-related changes in meridional wave transfer. For instance, in a region where

Γ becomes more negative, it indicates wave growth due to enhanced influxes of enstrophy (see section 2c of White *et al*., 2015).

2.2. Global data sets and statistical analysis

The reanalysis data sets used are from the National Centers for Environmental Prediction (NCEP) and include the Climate Forecast System Reanalysis (CFSR) for the period of 1979-2010 and its extension - the Climate Forecast System version 2 (CFSv2) - covering the period 2011-2017 (Saha *et al*., 2012). Jointly, they cover the 1979-2017 period (39 years in total). Both data sets were generated by NCEP's Climate Forecast System (CFS), which assimilates standard ground-based, radiosonde, and satellite observations into an atmosphere-ocean general circulation model with fully coupled atmosphere, land, ocean and sea ice components. Observed carbon dioxide, aerosols, other trace gases and solar variations are also included. Currently, CFSR and CFSv2 are the only reanalysis products directly providing isentropic level data at altitudes above 850 K (~10 hPa or 32 km).

The 6-hourly isentropic level data output at 2.5^{o} horizontal resolution on sixteen potential temperature levels from 270 K to 1500 K (equivalent to 900-2 hPa or 1-45 km) were obtained from http://rda.ucar.edu/datasets. Unlike previous studies that generated data on isentropic surfaces by interpolating 6-hrly pressure-level data provided by ECMWF (e.g. HH09; White *et al*., 2015; 2016), the isentropic level data used here were generated by NCEP as an integral part of the CFSR/CFSv2 reanalyses. The data used here involve no additional interpolation. All the diagnostics described in Section 2.1 are first calculated using daily averages of the 6-hourly fields before taking monthly and seasonal averages. The derivatives are calculated using centred differences except for the top and bottom isentropic levels where one-sided differences are used.

Previous studies suggest that the QBO defined by the tropical zonal winds near 40-50 hPa appears to optimize the stratospheric vortex response during NH winter (e.g. Holton and Tan, 1980; Lu *et al*., 2008; HH09; Gray *et al*., 2018). The monthly-averaged tropical zonal winds at 40 hPa and 50 hPa are obtained from radiosonde observations issued by the Freie Universität Berlin (Naujokat, 1986; FUB, 2016). Here, the easterly phase is defined for each individual month when the winds at both 40 hPa and 50 hPa are negative while the westerly phase is defined for each individual month when the equatorial winds at both pressure heights are positive. Additionally, the two years following the two major volcanic eruptions are excluded (i.e., El Chichón, March 1982 and Mount Pinatubo, June 1991). This results in eleven easterly QBO NH winters (i.e. 1979/80, 1981/82, 1984/85, 1989/90, 1996/97, 1998/99, 2003/04, 2005/06, 2007/08, 2012/13, 2014/15) and eighteen westerly QBO NH winters (i.e. 1980/81, 1985/86, 1987/88, 1988/89, 1990/91, 1993/94, 1995/96, 1997/98, 1999/00, 2002/03, 2004/05, 2006/07, 2008/09, 2010/11, 2011/2012, 2013/14, 2015/16, 2016/17). Note that there are more winters classified as wQBO than eQBO. This is because descending wQBO tends to stall and linger longer in the lower stratosphere while eQBO descends more quickly there. The dates listed may vary slightly from early to late winter as the QBO changes phase. Hereinafter the easterly and westerly QBO phase groups are denoted by eQBO and wQBO, respectively.

Note also that five wQBO winters coincide with ENSO events (i.e. 1997/98, 2002/03, 2004/05, 2006/07 and 2015/16) while only one eQBO winter was affected by a major ENSO event (i.e. 2014/15). We have carried out sensitivity tests by excluding those ENSO-affected winters and the results remain qualitatively the same (not shown).

The QBO signals are estimated based on the composite-mean differences between eQBO and wQBO subgroups (i.e. eQBO – wQBO). The statistical significance of eQBO – wQBO composite-mean differences is assessed using a Monte Carlo trial based non-parametric test. The procedure involves replacement of eQBO and wQBO composite members by randomly sub-sampling the original time series with replacement before averaging. This procedure is repeated 10,000 times and a distribution of the composite-mean differences is constructed. The original composite-mean difference estimated from the actual eQBO and wQBO subgroups is then compared with this distribution. When the actual positive (negative) difference is located within the upper (lower) 5% of the distribution, the difference is regarded as statistically significant and referred to as *the QBO signal*. Very similar results are obtainable based on Student's *t*-test (not shown).

3. Results

3.1. Mean-state and RWB responses

The climatological zonal-mean zonal winds $\overline{u}$ under eQBO and wQBO during November to January (Nov-Jan) and February to March (Feb-Mar) are shown in Fig. 1a-d. As expected, $\overline{u}$ in the NH is characterised by two westerly jets, i.e. the stratospheric polar vortex and the subtropical jet in the troposphere. The winter westerlies and summer easterlies are separated by the zero-wind line near the equator, where distinct differences between eQBO and wQBO are visible.

[[Insert Fig. 1 here]]

The QBO signal (i.e. eQBO – wQBO) in NH $\overline{u}$ during Nov-Jan is marked by easterly differences at high latitudes (up to −10 m s^{-1}) and westerly differences in the subtropics (~5 m s^{-1}) (Fig. 1e). Larger differences (~ ±35 m s^{-1}) can be found at the equator though the maximum/minimum color values in Fig. 1e, f have been capped to ±15 m s^{-1} in order to highlight

the extratropical responses. In late winter the sign of the response reverses, with westerly differences in the upper stratosphere at mid-high latitudes (~13 m s^{-1}) (Fig. 1f). Fig. 1 also indicate that the SWJ in the NH is weakened and/or shifted poleward under eQBO in late winter. These results are in good agreement with previous studies (Crooks and Gray, 2005; Garfinkel and Hartmann, 2011a; Lu *et al*., 2014; White *et al*., 2016; Zhang *et al*., 2019).

The corresponding QBO response of the zonal-mean temperature $\overline{T}$ is shown in Fig. 2. The QBO signal in extratropical $\overline{T}$ is marked by warm differences in the polar lower to middle stratosphere during Nov-Jan, and cold differences in the middle to upper stratosphere during Feb-Mar. At low latitudes, the QBO signal is marked by a vertical tripole structure in the tropics and a dipole pattern in the subtropics, which are associated with the QBO-MMC (Plumb and Bell, 1982). Similar to the QBO signals in $\overline{u}$ (Fig. 1e, f), these low-latitude QBO signals in $\overline{T}$ also persist throughout the winter.

[[Insert Fig. 2 here]]

Figs. 1e and 2a confirms that the HTE holds most robustly in early winter (e.g. Gray *et al*., 2004; 2018; Lu *et al*., 2008; 2014; White *et al*., 2016). The late winter response however differs in significance and magnitude in comparison with previous studies. For instance, a weaker HTE in the lowermost stratosphere rather than a full sign reversal was obtained if pre-1979 data were included (see Figures 1e, f of Lu *et al*., 2014). Lu *et al*. (2014) found that a late-winter weakening or reversal of the HTE during 1977-1998 was associated with a distinctly stronger and/or wider polar vortex around Nov-Jan.

Fig. 3 shows the eQBO and wQBO composites of the zonal-mean PV gradient $\overline{P}_\phi$ and the corresponding QBO composite differences during Nov-Jan and Feb-Mar. As expected, the climatological $\overline{P}_\phi$ is mostly positive during both eQBO and wQBO winters (Fig. 3a-d). Large values of $\overline{P}_\phi$ are found at low latitudes where RWs tend to be absorbed and near the westerly jets where RWs preferably propagate towards. In the extratropical NH, the most preferable route for the upward propagating PRWs is the polar vortex edge (i.e. grey dotted lines in Fig. 3e. f). In the subtropical to mid-latitude lower stratosphere, i.e. 25-60°N, 350-550 K, RWs preferably propagate towards the equator; an effect that is most pronounced for SRWs (Karoly and Hoskins, 1982). Relatively small values of $\overline{P}_\phi$ are found in the latitude band of 20-45°N in the middle stratosphere where the surf zone is formed as a result of RWB (McIntyre and Palmer, 1983; Hitchman and Huesmann, 2007).

[[Insert Fig. 3 here]]

The extratropical QBO signal in $\overline{P}_\phi$ is dominated by negative differences at 55-75°N, 450-1000 K during Nov-Jan and positive $\overline{P}_\phi$ differences at 55-75°N, 1250-1500 K during Feb-Mar. This reversal of the QBO signal between early and late winter is largely due to a reduction of $\overline{P}_\phi$ in the extratropical upper stratosphere under wQBO (Fig. 3d vs 3c). Reduction of $\overline{P}_\phi$ in these regions is most likely due to increased poleward RWB (Hitchman and Huesmann, 2007).

Positive QBO differences in $\overline{P}_\phi$ are found in the subtropical lower stratosphere near the eQBO-zero-wind line (Fig. 3e, f). These positive differences indicate enhanced PV gradients under eQBO and appear in both early and late winters. A similar effect can also been seen in the middle to upper

stratosphere at 15-30°N, ~850-1250 K during wQBO (Fig. 3c-d) but the magnitude is noticeably smaller than its lower-level counterparts under eQBO. In the QBO difference plots (Fig. 3e, f), these upper-level effects under wQBO is overpowered by those associated with eQBO. At 20-40°N, 400-550 K, $\overline{P}_\phi$ is larger during eQBO but smaller during wQBO. This implies that PRWs are more likely to propagate through the region and into the middle to upper stratosphere under eQBO.

Fig. 3 also shows that $\overline{P}_\phi$ near the equator becomes larger when the tropical winds are westerly but smaller when tropical winds are easterly. These QBO-related anomalies and those in the subtropical summer hemisphere are associated with barotropic instability of the subtropical easterly jet in the summer hemisphere, which occurs when the tropical winds are westerly (Hitchman *et al*., 1987). The unstable RWs generated via barotropic instability is further amplified by inertial instability near the equator (O'Sullivan and Hitchman, 1992). Breaking of these unstable waves acts to sharpen PV gradients at the equator (Hitchman and Huesmann, 2007), thus the rather large values of $\overline{P}_\phi$ at 10°S-10°N (Fig. 3a-d). These low-latitude QBO-signals display little seasonal variation.

We next examine RWB by showing the seasonal progression of the zonally-averaged frequency of the overturning PV gradient $\overline{\gamma}$ during eQBO and wQBO winters and the associated QBO composite differences from November to March (Fig. 4). $\overline{\gamma}$ is in general inversely proportional to $\overline{P}_\phi$, thus, opposite in sign to those shown in Fig. 3. This inverse relationship is due to dynamics, i.e. high PV gradients promote wave propagation (and hence less RWB) while mixing induced by RWB acts to smooth the background PV contours.

[[Insert Fig. 4 here]]

The key climatological features of $\overline{\gamma}$ are marked by regions with infrequent overturning of PV contours near the westerly jet core (i.e. the dotted lines in the extratropics) and at the equator, separated by a region with relatively large values of $\overline{\gamma}$ at 20-45°N (Fig. 4a-j). This region with noticeably more frequent reversals of PV contours (~10-15 days per month) signifies the so-called "surf zone". Frequent reversals of PV contours are also found in the subtropical summer stratosphere, reflecting barotropic instability of the subtropical easterly jet (Hitchman *et al*., 1987).

The differences in RWB between the two QBO phases in the extratropical winter hemisphere can be best appreciated by examining the seasonal evolution of the surf zone alongside with the polar vortex. During eQBO winters (Fig. 4a-e), the mid-latitude surf zone is mostly upright at 400-1000 K. $\overline{\gamma}$ at high latitudes at 60-70°N does not show strong seasonal variation from December through March either (Fig. 4b-e). Also, $\overline{\gamma}$ typically takes values ranging between 8 to 10 days per months near the polar vortex edge, which is not much smaller than those found in the surf zone. Fig. 4a-e thus suggests that RWB in the middle to upper stratosphereduring eQBO winters does not involve a gradual sharpening of PV gradients near the polar vortex edge.

In contrast, under wQBO, the surf zone in the middle to upper stratosphereis vertically connected with the surf zone in the lower stratosphere (Fig. 4f-j). The surf zone as a whole tilts equatorward with height in early winter (Fig. 4f-g), becomes upright in January (Fig. 4h), then tilts towards the North Pole in late winter (Fig. 4i-j). In addition, $\overline{\gamma}$ near the polar vortex edge gradually increases from under 4 days per month in November to over 12 days per month in March (Fig. 4f-j). These results suggest that RWB-related mixing is confined to the surf zone in the early winter but gradually works its way poleward in late winter. Fig. 4k-o shows that a sign reversal of the $\overline{\gamma}$

differences between the two QBO phases occurs around February, coinciding with the reversal of the HTE in the upper stratosphere in late winter (see Figs. 1f and 2b).

The QBO signal in the subtropical upper stratosphere of the NH is most strong in early winter (Fig. 4k-l). This is due to a northward and downward shift of the PRW absorption region during wQBO (Fig. 7b, e vs 7a, d). In November, the region with relatively large values of $\overline{\gamma}$ is located at 5-20°N, 1000-1500 K during eQBO (Fig. 4a) but become more poleward and downward at 20-40°N, 850-1250 K under wQBO (Fig. 4f). The negative $\overline{\gamma}$ differences centred at 25°N, 1250 K persist from November to February due to more frequent RWB in the surf zone under wQBO (Fig. 4k-o). The positive differences centred at 10°N, 1500 K are paired with negative differences centered at 5°S, 1500 K, indicating a southward shift of the wave absorption during wQBO or northward shift of the wave absorption region during eQBO. These effects disappear since December, indicating that wave absorption at the low-latitude stratopause is affected by the QBO only in early winter.

Negative QBO differences in $\overline{\gamma}$ are also found in the lower stratosphere at 15-40°N, 400-550 K, which show little evidence of poleward migration or seasonal variation (Fig. 4k-o). The positive $\overline{\gamma}$ differences in the subtropical summer hemisphere in Fig. 4k-o are associated with the barotropic instability of the easterly jet due to the relocated zero-wind line by the QBO (O'Sullivan and Hitchman, 1992; HH09).

To better understand the QBO modulation of RWB in the middle to upper stratosphere, Fig. 5 shows scatterplots of PV gradient $\overline{P}_\phi$ vs $\overline{\gamma}$ in the mid- to upper stratospheric surf zone, i.e. 25-40°N, 850-1250 K for 2-month over-lapping running averages from October to January. As we

expect, $\overline{P}_\phi$ (i.e. the strength of the waveguide) and $\overline{\gamma}$ (i.e. the frequency of RWB) are anti-correlated, which is consistent with the dissipative effect of RWB. However, $\overline{\gamma}$ is noticeably larger under wQBO than eQBO for a given value of $\overline{P}_\phi$. Such enhancement is most strong in early winter (i.e. Oct – Nov, Fig. 5a-b), during which the correlation between $\overline{\gamma}$ and $\overline{P}_\phi$ is statistically significant under wQBO ($r = -0.71$, $p \leq 0.05$) but fails to pass the statistical test under eQBO ($r = -0.37$, $p = 0.23$). These results confirm enhanced RWB under wQBO in the middle to upper stratosphere with strong mixing in the mid-latitude surf zone in early to middle winter. Thus, the preferable location and the seasonal development of RWB appear to be modulated by the QBO.

[[Insert Fig. 5 here]]

3.2. Changes in wave mean-flow interaction

In this section, we examine the QBO modulation of wave-driving based on the EP fluxes and the density-weighted eddy PV fluxes Π. Previous studies have suggested that the HTE involves changes in PRWs as well as SRWs (e.g. Garfinkel *et al*., 2012; White *et al*., 2016). To examine their relative contributions, the analysis of Fig. 6 is repeated but separately for zonal wavenumber 1 (wave-1), zonal wavenumbers 2-3 (wave-2-3) and for zonal wavenumbers 5-10 (SRWs). These wave forcing analyses are performed for Nov-Dec and Feb-Mar, in order to highlight the early and late winter differences.

Fig. 6a-b shows the early and late winter climatology of the EP fluxes (arrows) and the density-weighted eddy PV flux $\Pi = \overline{\sigma \hat{v} \hat{P}^*}$ (contours); the latter is equivalent to the EP flux divergence $(a\cos\phi)^{-1}\tilde{\nabla}\cdot\tilde{\mathbf{F}}$. The climatology of PRW propagation throughout the winter stratosphere is marked

by upward pointing and equatorward tilted EP flux vectors (see Fig. 3a-d). Π is mostly negative (i.e. the converging EP fluxes) and centred at the polar vortex edge. The few small regions with positive Π near the equator and on the poleward flank of the westerly jets indicate internal wave generation, most likely due to localized instability (e.g. Simmons and Hoskins, 1978).

[[Insert Fig. 6 here]]

The early winter QBO signal in Π (Fig. 6c) is characterized by convergent EP flux anomalies at high-latitudes, i.e. negative Π differences poleward of 50°N and in the subtropical lower stratosphere at 20-40°N, 400-650 K. These Π anomalies are accompanied by enhanced upward EP flux vectors north of ~55°N and equatorward and poleward pointing EP flux vectors in the lower stratosphere. These EP flux anomalies indicate enhanced upward propagating and stronger wave forcing on the polar vortex, which is consistent with a weaker polar vortex in early winter during eQBO. Positive Π differences that are of relatively smaller amplitude are found at 20-45°N, 700-1250 K, where the mid- to upper stratospheric surf zone is located. The anomalous EP flux divergences there can be linked to RWB, which is enhanced during wQBO (Figs. 4 and 5).

In late winter, the wave forcing response at high-latitudes reverses the sign, i.e. larger negative values of Π near the polar vortex edge are found to associate with wQBO (Fig. 6d). This is consistent with a weaker polar vortex during wQBO and enhanced RWB in the middle to upper stratosphere where the wave forcing gradually expands from the surf zone into the high latitudes (see Figs. 1f, 2b, and 4f-j).

In the subtropics, the QBO signal in Π is marked by negative differences in the lower stratosphere and positive difference in the middle to upper stratosphere. These subtropical QBO signals are present in both early and late winter in association with the QBO-zero wind lines. These

QBO signals are accompanied by enhanced equatorward or poleward EP flux vectors in response to more positive or negative $\overline{P}_{\phi}$ northward of the corresponding QBO-zero-wind lines (Fig. 3e, f).

QBO modulation of wave forcing is separately into three bands of zonal wavenumbers and the Nov-Dec averages are shown in Fig. 7 while those for Feb-Mar averages are shown in Fig. 8. It is evident that the QBO modulation of Π is dominated by PRWs while SRWs play a relatively minor role, except near the SWJ where the EP flux vectors are noticeably large. Several regions of positive Π are featured and include the effects from both PRWs and SRWs, implying that instability and/or nonlinear wave-wave interactions might be involved. The exact role of nonlinearity is however complex and cannot be properly studied using seasonal averages or the zonal mean fields. It is thus beyond the scope of this paper but will be a subject of future studies.

[[Insert Figs. 7 and 8 here]]

Figs. 7 and 8 suggests a complex interplay among wave-1, wave-2-3 and SRWs. In early winter, a weaker polar vortex during eQBO is largely due to enhanced wave-1 forcing in the middle to upper stratosphere, where these waves are guided upward along the polar vortex edge (Fig. 7a-c). There is ~25% increase in wave-1 EP-flux convergence during eQBO in comparison to those during wQBO. Divergent differences of wave-2-3 are found at 20-50°N, 850-1250 K with meridional EP fluxes vectors that point equatorward and poleward near the surf zone (Fig. 7f). These wave-2-3 anomalies are nevertheless of smaller magnitude than those associated with wave-1 (1.8 m s^{-1} day^{-1} versus 2.8 ms^{-1} day^{-1}). In the lower stratosphere and during eQBO winters, extratropical PRWs are refracted equatorward while they pass a region with small or even close to zero PV gradient at 25-45°N, 350-650 K (see Fig. 3). Wave-2-3 anomalies appear to be generated internally and reflected poleward, indicated by the poleward pointing EP flux vectors and convergent differences of wave-

2-3 at 55-80°N, 400-650 K (Fig. 7f). Thus, RWB in the lower stratosphere may involve wave activity transfer from wave-1 to wave-2-3 likely due to nonlinear evolution of a Rossby wave critical layer with barotropical instability (Haynes, 1989).

SRWs are generated on the equatorward flank of the polar vortex and dissipate sideways in the middle to upper stratosphere at 700-1500 K during both eQBO and wQBO (Fig. 7g, h). This effect is significantly stronger and deeper in altitude during wQBO. Using a single-layer barotropic model, Scott (2019) studied meridional wave transfer between two waveguides in the winter stratosphere. It was found that the latitudinal separation between the high- and low-latitude waveguides is effectively reduced locally due to finite amplitude wave disturbances or nonlinear RWB. Wave activity transfer from PRWs to SRWs is noticeably enhanced when the low-latitude waveguide is located in the winter hemisphere. Fig. 7d-i confirms that this nonlinear effect becomes stronger in the middle to upper stratosphere during wQBO winters.

In late winter, the convergent wave-1 differences become noticeably weaker and more confined to the high latitudes at 65-85°N, 350-1250 K (Fig. 8c). During eQBO, convergence of wave-1 remains strong in the upper stratosphere poleward of 35°N (Fig. 8a), which is similar to those in early winter (Fig. 7a). During wQBO, the wave-1 forcing is centred at the polar vortex edge and extends downward into the lower stratosphere (Fig. 8b). The latitudinally alternating negative, positive and negative differences in Fig. 8c are merely due to a more poleward and downward shift of the wave-1 forcing during wQBO. A weakened wave-1 response to the QBO in late winter has also been found by Zhang *et al*. (2019), who throughoutly examined QBO modualtion of wave-1 and its seasonal evolution in weakening and displacing the polar vortex.

The QBO signal in wave-2-3 forcing during late winter is marked by the positive Π differences on both flanks of the polar vortex at 20-55°N, 850-1500 K and at 60-80°N, 350-1000 K (Fig. 8f). These divergent anomalies of wave-2-3 are accompanied by significantly reduced wave-2-3 from the troposphere at 35-70°N. We noted that the absolute values of Π and $F^{(\theta)}$ associated with wave-2-3 in the affected regions during wQBO is near twice as large as those under eQBO (Fig. 8e vs Fig. 8d). Thus, the late-winter changes in wave forcing is dominated by PRWs of wave-2-3.

Fig. 9a shows scatter plot between Jan-Mar averaged vertical component of the EP fluxes $F^{(\theta)}$ of wave-2-3 at 35-70°N, 350-450 K (x-axis) and the meridional component of EP-flux divergence $\Pi_\phi = (a\cos\phi)^{-2}\frac{\partial}{\partial\phi}\left(\tilde{F}^{(\phi)}\cos\phi\right)$ of wave-2-3 at 20-40°N, 850-1500 K (y-axis). These two regions are chosen because PRWs of wave-2-3 normally propagate upward from the troposphere into the stratosphere at 35-70°N while the most significant QBO signal of wave-2-3 is in the subtropical to middle latitude upper stratosphere at 20-40°N, 850-1500 K (see Figs. 7-8). It is evident that these two quantities are negatively correlated regardless of the QBO (r = -0.57, p = 0.002). However, $F^{(\theta)}$ is generally more positive and Π_ϕ is more negative during wQBO than eQBO. When $F^{(\theta)}$ is relatively small, Π_ϕ is noticeably more negative during wQBO than eQBO for a given value of $F^{(\theta)}$. These results suggest enhanced RWB in the middle to upper stratosphere during wQBO winters is accompanied by enhanced upward propgation of wave-2-3 from the lower stratosphere. The connection is weakened during eQBO. Weaker but qualitatively similar results can be obtained in early and middle winters (not shown).

However, QBO differences in upward propagating wave-2-3 $F^{(\theta)}$ is only statistically signficant in late winter. To understand this, Fig. 9b shows scatter plot between the vertical component of the

wave-2-3 EP fluxes $F^{(\theta)}$ during Jan-Mar at 35-70°N, 350-450 K (y-axis) and the Dec-Feb mean meridional component of wave-2-3 EP-flux divergence Π_ϕ at 35-70°N, 350-650 K (x-axis) in the lower stratosphere. Regardless of the QBO, $F^{(\theta)}$ is positively correlated with Π_ϕ (r = 0.46, p = 0.004), suggesting upward propogation of wave-2-3 is enhanced when meridional divergence of wave-2-3 in the extratropical lower stratosphere is large and vice versa. This correlation however becomes much weaker if Jan-Mar averaged is used for Π_ϕ (not shown). A one-month lag required between $F^{(\theta)}$ and Π_ϕ implies that the relevant process is cumulative. Fig. 9 also suggests that this lagged relationship between $F^{(\theta)}$ and Π_ϕ is noticeably enhanced durng wQBO (r = 0.68, p = 0.001) but statistically insignificant during eQBO. We suggest that finite amplitude transient wave-2-3 in association with RWB in the lower stratosphere hinders baroclinic growth of wave-2-3 from below. This effect is stronger during eQBO due to enhanced RWB in the lower stratosphere. During wQBO, the polar vortex response to the wave-2-3 fluxes from below involves successive RWB events that extends from the upper-level to the lower stratosphere. Downward expansion of RWB is strong around January, thus enhanced wave-2-3 response in the lower stratosphere in late winter.

[[Insert Fig. 9 here]]

3.3. Down-gradient eddy PV fluxes

RWB-related eddy PV fluxes are typically directed down the background PV gradients in the winter stratosphere (see Sec. 2.1). From Figs. 7-9, we expect this effect to be more pronounced in the middle to upper stratospheric surf zone in early winter and then progresses into lower stratosphere in middle winter under wQBO. In this section, we focus on the Nov-Jan period to demonstrate such an effect.

Fig. 10a shows the climatology of down-gradient eddy PV flux Γ averaged over Nov-Jan when all wavenumbers are included. As expected, Γ is mostly negative in the extratropical winter stratosphere, except for a few small regions on the poleward flank of the tropospheric subtropical jet and in the polar stratosphere where instability, nonlinear wave-wave interaction and/or upscaling play a role (e.g. Birner *et al*., 2013).

[[Insert Fig. 10 here]]

The corresponding QBO differences in Γ are shown in Fig. 10b, c, where the responses are separated into November and Dec-Jan averages so that a poleward and downward movement of Γ anomalies can be examined. In November, the extratropical response is characterized by negative Γ differences on the poleward flank of the polar vortex and positive differences on its equatorward flank (Fig. 10b). The negative Γ differences poleward of 55°N indicate enhanced down-gradient eddy PV fluxes during eQBO, corresponding to the enhanced wave-1 forcing in the same region (Fig. 7c). The positive Γ differences 35-55°N, 850-1500 K are associated with increased RWB during wQBO, corresponding to meridional EP flux convergence of wave-2-3 forcing in the same region (Figs. 7f and 8f). In Dec-Jan, the positive Γ differences intensify and extend poleward and downward into the lower stratosphere while the negative differences of Γ at high latitudes disappear (Fig. 10c). These Γ differences confirm the importance of wave-1 disturbances during early winter and a more persistent, poleward and downward expansion of wave-2-3 contribution during wQBO.

3.4. Unique features of the QBO responses

Polar vortex variability can be associated with anomalous RWB without the influence of the QBO. Previous studies have showed feedbacks within the stratosphere are strong and can

overwhelm the initial perturbation provided by the QBO (Watson and Gray, 2014). It is helpful to examine the extent to which the QBO-related differences are distinct from those during weak versus strong vortex states. In the reanalyses, a composite of weak vortices is necessarily affected by eQBO in early winter while a composite of strong vortex winters would be biased towards wQBO. The HTE is relatively weak in February, permitting an assessment to be made between the QBO signals and those associated with extreme vortex states.

The same set of analyses shown in sections 3.1-3.3 are thus repeated by compositing weak- and strong-vortex states using zonal-mean zonal winds near the polar vortex edge in February. A weak (strong) polar vortex in February is defined when the averaged winds at 45-75°N, 450-1500 K is smaller (or greater) than their mean value over the 1979-2017 period minus (or plus) half of its standard deviation. No significant zonal wind differences are detected in the tropics between these two vortex states; the extratropical differences between these two vortex states are thus effectively independent of the QBO (not shown).

It can be shown that weak vortex is generally associated with an enhanced poleward pointing waveguide in the subtropics. A strong-vortex state is associated with a distinct waveguide along the polar vortex edge with a well-defined surf zone in the mid-latitudes. Thus, the QBO-related waveguide and RWB differences measured by $\overline{P}_{\phi}$ and $\overline{\gamma}$ in the extratropical stratosphere are effectively associated with the two extreme vortex states. In terms of wave forcing, the weak- (or strong-) vortex state is associated with enhanced (or reduced) PRWs from the troposphere. Distinct and persistent QBO-related changes are largely confined to the subtropics while the extratropical responses to the QBO are similar to the weak-vs-strong vortex states. These results suggest that the

HTE and its relevant mechanism(s) may not be properly examined using $\overline{P}_{\phi}$, $\overline{\gamma}$ and/or the divergent field of the total EP fluxes.

The QBO-related responses become distinct when wave mean-flow interaction is examined according to wavenumbers and their seasonal development. In the context of the HTE, the QBO-related features include: 1) the enhanced upward wave-1 anomalies and absorption of those waves in the extratropical stratosphere during eQBO; 2) the "fountain-like" structure of EP flux anomalies in the lower stratosphere with convergent anomalies in the subtropics and at high latitudes during eQBO; 3) meridional convergent wave-2-3 anomalies at 20-40°N, 850-1500 K during wQBO; and 4) a gradual build-up and enhancement of upward wave-2-3 anomalies at 35-70°N during wQBO.

3.5. The role of the QBO-MMC

To understand how the QBO-MMC may be linked to the HTE, Fig. 11 shows meridional velocity $\overline{v}$ over the latitude-height cross section of 30°S-40°N and 400-1500 K during November for eQBO and wQBO averages and corresponding QBO differences. The QBO-MMC with its NH divisions is indicated by the blue arrows in Fig. 11a-b, which is aligned with the positions of the maxima and minima QBO-related $\overline{v}$ differences below 1000 K (Fig. 11c). The northward circulation in the subtropical NH (i.e. 5-25°N) is enhanced at ~600 K (50 hPa) under eQBO but at ~400 K (100 hPa) and ~850 K (10 hPa) under wQBO.

[[Insert Fig. 11 here]]

The largest QBO signal in $\overline{v}$ is in fact in the middle to upper stratosphere at ~0-30°N, 850-1250 K, in association with an enhanced northward and downward motion of the equatorial winds during wQBO, indicated by the purple arrow in Fig. 11b. This downward motion and the cross-

equatorial flow are known to be sensitive to the semi-annual oscillation (SAO), a dominant feature of equatorial winds in the upper stratosphere and lower mesosphere (Hitchman and Leovy, 1986; Smith *et al*., 2017).The SAO is strongly coupled with wQBO in November when the SAO is in its westerly phase (Smith *et al*., 2017). This may play a role in enhanced RWB in the upper stratosphere during early winter under wQBO.

PV gradients in the subtropical stratosphere become more positive where the QBO-MMC and/or SAO-MMC are directed poleward in the same height region (Fig. 3). Thus, the QBO-MMC and/or SAO-MMC may play a role in altering the subtropical waveguide whereby they contribute to the enhanced RWB in the affected layers.

4. Conclusions and Discussion

Motivated by the observed intra-seasonal dependence in the HTE, this tropical-extratropical connection is re-examined here by focusing on QBO modulation of RWB. Based on the NCEP-CFS reanalysis data sets in isentropic coordinates that covers the 1979 – 2017 period, we have studied QBO-related changes in zonal-mean circulation, waveguide, frequency of overturning PV contours, the net wave forcing of the stratosphere as well as the QBO-MMC. Our results suggest RWB is generally enhanced in the height region where the QBO zero-wind line is shifted into the NH and/or where the secondary meridional circulation associated with the QBO or the SAO are directed northward. The enhancement is accompanied by more positive PV gradients in the subtropics. In this context, the classic HT mechanism, i.e. QBO induces changes in the total volume or width of stratospheric waveguide whereby it regulates the net wave forcing on the polar vortex, remains valid. Our results further confirm that QBO modulation of extratropical wave activity is wavenumber-dependent. Instead of a static alteration of the total wave forcing, QBO modulation of

RWB results in changes in both waveguide and wave structure throughout the winter season. The polar-vortex response thus switches from reinforcement to disturbance around February due to a gradual build-up of upward propagating wave-2-3 during wQBO. These results suggest that examining the total EP fluxes and divergence alone cannot adequately explain the observed HTE. Results solely based on mid-winter averages can be potentially misleading due to cancellation between wave-1 and wave-2-3 responses.

RWB is intrinsically nonlinear and sensitive to both background flow and the wave forcing from below (Polvani and Saravanan, 2000; Scott and Dritschel, 2005). It acts to reshape the background waveguide and alter the wave structure via nonlinear wave transfer (Waugh and Dritschel, 1999; Scott, 2019). Fig. 12 depicts a schematic diagram that highlights our key findings in the context of the HTE. During eQBO winters (Fig. 12a,b), an increase in upward propagating PRWs of wave-1 and absorption of those waves in the mid- to high-latitude stratosphere plays a major role in a disturbed polar vortex. RWB is also enhanced in the lower stratosphere. In early winter (Fig. 12a), RWB acts to strengthen the background PV gradients at 20-40°N, permitting more PRWs to the winter stratosphere. The enhanced upward PRWs and RWB form a "fountain-like" feature of EP-flux anomalies in the lower stratosphere with convergent anomalies in the subtropics and at high latitudes. Thus, SSWs are more likely to occur in early winter during eQBO.

[[Insert Fig. 12 here]]

In late winter, upward propagating wave-1 remains enhanced. However, as more PRWs entering the stratosphere, RWB in the lower stratosphere intensifies and becomes nonlinear. Nonlinear wave activity transfer in association with RWB leads to growth of transient waves of wave-2-3 and SRWs (Scott, 2019). Breaking of SRWs acts to enhance the background PV gradient (Garfinkel *et al*.,

2012; White *et al*., 2015). Transient wave-2-3 of finite amplitudes hinders baroclinic growth of quasi-stationary wave-2-3 from below, i.e. the blue vertical arrows in Fig. 12b. The net wave forcing on the polar vortex is thus weakened due to reduced wave-2-3 forcing.

During wQBO winters, RWB is preferably enhanced in the middle to upper stratosphere and the effect is dominated by wave-2-3 (Figs. 12c, d). In early winter (Fig. 12c), RWB is confined to the upper-level where it acts to sharpen PV gradients on the equatorial flank of the polar vortex with frequent overturning of PV contours in the surf zone at 20-40°N, 850-1500 K. Down-gradient wave activity in the surf zone is accompanied by reduced wave disturbances at high latitudes and below 850 K. The polar vortex thus remains stable while the westerly winds in the upper-level weaken and then reform periodically in response to RWB. As the winter progresses, upward propagating PRWs of wave-2-3 gradually gain strength due to "pre-conditioning" and successive RWB events. Around January, the entire polar vortex becomes ‘eroded’ by RWB as a result of a poleward confinement and downward extension of wave activity. Thus, SSWs are more likely to occur in late winter during wQBO (Fig. 12d). These wQBO-related processes appear to be generic to a strong-vortex state in which RWB is initially confined to the upper stratosphere (Waugh and Dritschel, 1999; Polvani and Saravanan, 2000).

The correlation between the QBO and the polar vortex strength has been found to vary on decadal to multi-decadal time-scales (Gray *et al*., 2004; Lu *et al*., 2008; 2014). This is again expected due to wave-2-3 anomalies involve nonlinear wave activity transfer via RWB. The seasonal development of RWB is affected by the state of the polar vortex while the net wave forcing of the stratosphere is sensitive to the state of RWB. The observed HTE may liaise with other processes, such as solar forcing, snow cover and ENSO, which can bring about characteristic

changes in RWB and its seasonal evolution. For instance, El Nino events occurred more often when the QBO was in its westerly phase in recent decades, which would have contributed to a weaker-than-expected ENSO signal in the winter stratosphere (Domeisen *et al*., 2019). Likewise, ultra-violet solar irradiance alters wave mean-flow interaction in the upper stratosphere and the structure of PRWs from below can be altered by ENSO and snow-cover over Eurasian (Lu *et al*., 2017; Cohen and Entekhabi, 1999; Peings *et al*., 2017). Given the relatively short period under consideration (i.e. 1979-2017), uncertainties are expected in terms of the magnitudes of the responses and the timing of late winter reversal.

Acknowledgements: This study is part of the British Antarctic Survey (BAS) Polar Science for Planet Earth programme and the National Centre for Atmospheric Science (NCAS) of the Natural Environment Research Council (NERC). HL, LJG and SO were supported by the NERC North Atlantic Climate System Integrated Study (ACSIS) (NE/N018028). SO and LJG were also partially supported by the NERC grant NE/P006779/1. MHH was supported by the National Science Foundation grant AGS-1555851. We acknowledge use NCEP CFSR reanalysis data on isentropic coordinates (https://www.ncdc.noaa.gov/data-access/)

References:

Abatzoglou, J.T. and Magnusdottir G. (2007). Wave breaking along the stratospheric polar vortex as seen in ERA-40 data. *Geophys. Res. Lett*., 34, L08812.

Albers, J.R. and Birner, T. (2014). Vortex preconditioning due to planetary and gravity waves prior to stratospheric sudden warmings. *J. Atmos. Sci.,* 71, 4028–4054.

Andrews, D.G., Holton, J.R. and Leovy, C.B. (1987). Middle Atmosphere Dynamics. Academic Press, Cambridge, MA.

Andrews, M.B., Knight, J.R., Scaife, A.A., Lu, Y., Wu, T., Gray, L.J., & Schenzinger, V. (2019). Observed and simulated teleconnections between the stratospheric Quasi-Biennial Oscillation and Northern Hemisphere winter atmospheric circulation. *J. Geophys. Res*., 124, 1219–1232.

Anstey, A. and Shepherd, T.G. (2014). High-latitude influence of the quasi-biennial oscillation. *Quart. J. Roy. Meteor. Soc.*, 140, 1–21.

Baldwin, M.P., *et al.* (2001). The quasi-biennial oscillation. *Rev. Geophys.*, 39(2), 179–229.

Baldwin, M.P. and Dunkerton, T.J. (1999). Propagation of the Arctic Oscillation from the stratosphere to the troposphere. *J. Geophys. Res*. 104, 30937–30946.

Birner, T., Thompson, D.W. J. and Shepherd, T.G. (2013). Up-gradient eddy fluxes of potential vorticity near the subtropical jet. *Geophys. Res. Lett.*, 40, 5988-5993.

Butchart, N. *et al.* (2018). Overview of experiment design and comparison of models participating in phase 1 of the SPARC Quasi-Biennial Oscillation initiative (QBOi), *Geosci. Model Dev*., 11, 1009-1032.

Calvo, N., Giorgetta, M.A. and Peña‐Ortiz, C. (2007). Sensitivity of the boreal winter circulation in the middle atmosphere to the quasi‐biennial oscillation in MAECHAM5 simulations, *J. Geophys. Res.*, 112, D10124.

Cohen, J., and D. Entekhabi (1999). Eurasian snow cover variability and northern hemisphere climate predictability, *Geophys. Res. Lett*., 26(3), 345–348, doi:10.1029/1998GL900321.

Crooks, S. A., and Gray, L.J. (2005). Characterization of the 11-year solar signal using a multiple regression analysis of the ERA-40 dataset. *J. Clim.*, 18, 996–1015.

Domeisen, D.I., Garfinkel, C.I. and Butler, A.H. (2019). The teleconnection of El Niño Southern Oscillation to the stratosphere. *Rev. Geophys*, 57, 5– 47.

Dunkerton, T.J. and Baldwin, M.P. (1991). Quasi-biennial modulation of planetary-wave fluxes in the Northern Hemisphere winter. *J. Atmos. Sci.*, 48, 1043-1061.

FUB (2017). Freie Universität Berlin: The Quasi-Biennial-Oscillation (QBO). Data Series. http://www.geo.fu-berlin.de/en/met/ag/strat/produkte/qbo/. Accessed: 2017-07-11.

Garfinkel, C.I., Hartmann, D.L. (2011a). The influence of the Quasi-Biennial Oscillation on the troposphere in winter in a hierarchy of models. Part I: Simplified dry GCMs. *J. Atmos. Sci*., 68, 2026–2041.

Garfinkel, C.I., and Hartmann, D.L. (2011b). The influence of the Quasi-Biennial Oscillation on the troposphere in winter in a hierarchy of models. Part II: Perpetual winter WACCM runs. *J. Atmos. Sci*., 68, 1273-1289.

Garfinkel, C.I., Schwartz, C., Domeisen, D.I.V., Son, S.-W., Butler, A.H. and White, I.P. (2018). Extratropical atmospheric predictability from the quasi-biennial oscillation in subseasonal forecast models. *J. Geophys. Res.* 123, 7855–7866.

Garfinkel, C.I., Shaw, T.A., Hartmann, D.L. and Waugh, D.W. (2012). Does the Holton-Tan mechanism explain how the quasi-biennial oscillation modulates the Arctic polar vortex? *J. Atmos. Sci.*, 69, 1713-1733.

Geller, M.A. *et al.* (2016). Modeling the QBO: Improvements resulting from higher model vertical resolution. *J. Adv. Model. Earth Syst.*, 8, 1092–1105.

Gray, L.J., Anstey, J.A., Kawatani, Y., Lu, H., Osprey, S. and Schenzinger, V. (2018). Surface impacts of the Quasi Biennial Oscillation. *Atmos. Chem. Phys*., 18, 8227-8247.

Gray, L.J., Crooks, S., Pascoe, C., Sparrow, S. and Palmer, M. (2004). Solar and QBO influences on the timing of stratospheric sudden warmings. *J. Atmos. Sci.,* 61, 2777–2796.

Gray, L.J. *et al.* (2010). Solar influence on climate. *Rev. Geophys.*, 48, RG4001, doi:10.1029/2009RG000282.

Gray, L.J., Sparrow, S., Juckes, M., O'Neill, A. and Andrews, D.G. (2003). Flow regimes in the winter stratosphere of the northern hemisphere. *Quart. J. Roy. Meteor. Soc.*, 129, 925-945.

Haynes, P. H. (1989). The effect of barotropic instability on the nonlinear evolution of a Rossby wave critical layer. *J. Fluid Mech*., 207, 231–266.

Hitchman, M.H. and Huesmann, A.S. (2007). A seasonal climatology of Rossby wave breaking in the layer 330-2000 K. *J. Atmos. Sci.*, 64, 1922-1940.

Hitchman, M.H. and Huesmann, A.S. (2009). Seasonal influence of the quasi-biennial oscillation on stratospheric jets and Rossby wave breaking. *J. Atmos. Sci.*, 66, 935-946.

Hitchman, M.H., Gille, J.C. and Bailey, P.L. (1987). Quasi-stationary, zonally asymmetric circulations in the equatorial lower mesosphere. *J. Atmos. Sci*., 44, 2219–2236.

Hitchman, M.H. and Leovy, C.B. (1986). Evolution of the zonal mean state in the equatorial middle atmosphere during October 1978–May 1979. *J. Atmos. Sci*., 43, 3159–3176.

Holton, J.R. and Tan, H.C. (1980). The influence of the equatorial quasi-biennial oscillation on the global circulation at 50mb. *J. Atmos. Sci.*, 37, 2200-2208.

Holton, J.R. and Tan, H.C. (1982). The quasi-biennial oscillation in the Northern Hemisphere lower stratosphere. *J. Met. Soc. Japan*, 60, 140–148.

Hoskins, B.J., McIntyre, M.E. and Robertson, A.W. (1985). On the use and significance of isentropic potential vorticity maps. *Quart. J. Roy. Meteor. Soc.*, 111, 877-946.

Hu, Y. and Tung, K.K. (2002). Tropospheric and equatorial influences on planetary-wave amplitude in the stratosphere. *Geophys. Res. Lett*., 29(2), 1019.

Karoly, D. and Hoskins, B.J. (1982). Three-dimensional propagation of planetary waves. *J. Met. Soc. Japan,* 60, 109–123.

Kidston, J, Scaife, A.A., Hardiman, S.C., Mitchell, D.M., Butchart, N., Baldwin, M.P. and Gray, L.J. (2015). Stratospheric influence on tropospheric jet streams, storm tracks and surface weather. *Nat. Geo.*, 8(6), 433-440.

Killworth, P.D. and McIntyre, M.E. (1985). Do Rossby-wave critical layers absorb, reflect or over-reflect? *J. Fluid Mech*., 161, 449–462.

Kodera, K. (1994). Influence of volcanic eruptions on the troposphere through stratospheric dynamical processes in the northern hemisphere winter, *J. Geophys. Res.*, 99(D1), 1273–1282.

Labe, Z., Peings, Y., and Magnusdottir, G. (2019). The effect of QBO phase on the atmospheric response to projected Arctic sea ice loss in early winter. *Geophys. Res. Lett.*, 46, 7663–7671.

Labitzke, K. (1982). On the interannual variability of the middle stratosphere during the Northern Winters. *Quart. J. Roy. Meteor. Soc.*, 60(1), 124–139.

Lait, L.R. (1994). An alternative form for potential vorticity. *J. Atmos. Sci.*, 51, 1754-1759.

Leovy, C.B., Sun, C.-R., Hitchman, M.H., Remsberg, E.E., Russell III, J.M., Gordley, L.L., Gille, J.C. and Lyjak, L.V. (1985). Transport of ozone in the middle stratosphere: Evidence for planetary wave breaking. *J. Atmos. Sci*., 42, 230–244.

Limpasuvan V., Thompson D. W. J., and Hartman D. L. (2004). The life cycle of the Northern Hemisphere sudden stratospheric warmings, *J. Clim.*, 17, 2584–2596.

Lu, H., Baldwin, M.P., Gray, L.J. and Jarvis, M.J. (2008). Decadal-scale changes in the effect of the QBO on the Northern stratospheric polar vortex. *J. Geophys. Res.*, 113, D10114.

Lu, H., Bracegirdle, T.J., Phillips, T., Bushell, A.B. and Gray, L.J. (2014). Mechanisms for the Holton-Tan relationship and its decadal variation. *J. Geophys. Res.*, 119, 2811-2830.

Lu, H., Gray, L.J., White, I.P. and Bracegirdle, T.J. (2017). Stratospheric response to the 11-yr solar cycle: Breaking planetary waves, internal reflection, and resonance. *J. Clim.,* 30, 7169–7190.

Marshall, A.G. and Scaife A.A. (2009). Impact of the QBO on surface winter climate. *J. Geophys. Res.*, 114, D18110.

Matsuno, T. (1971). A dynamical model of the stratospheric sudden warming. *J. Atmos. Sci.,* 28, 1479–1494.

McIntyre, M.E. (1982). How well do we understand the dynamics of stratospheric warmings? *J. Meteor. Soc. Japan*, 60, 37–65.

McIntyre, M.E. and Palmer, T.N. (1983). Breaking planetary waves in the stratosphere. *Nature*, 305, 593-600.

McIntyre, M.E. and Palmer, T.N. (1984). The surf zone in the stratosphere. *J. Atmos. Terr. Phys*., 46(6), 825-849.

Naito, Y. and Yoden, S. (2006). Behavior of planetary waves before and after stratospheric sudden warming events in several phases of the equatorial QBO. *J. Atmos. Sci.*, 63, 1637–1649.

Nakamura, T., K. Yamazaki, K. Iwamoto, M. Honda, Y. Miyoshi, Y. Ogawa, Y. Tomikawa, and J. Ukita (2016). The stratospheric pathway for Arctic impacts on midlatitude climate, *Geophys. Res. Lett*., 43, 3494–3501, doi: 10.1002/2016GL068330.

Naoe, H. and Shibata, K. (2010). Equatorial quasi-biennial oscillation influence on northern winter extratropical circulation. *J. Geophys. Res*., 115, D19102.

Naujokat, B. (1986). An Update of the Observed Quasi-Biennial Oscillation of the stratospheric winds over the tropics. *J. Atmos. Sci*., 43(17), 1873-1877.

Osprey, S., Geller, M. and Yoden, S. (2018). The stratosphere and its role in tropical teleconnections. *Eos*, 99, doi: 10.1029/2018EO097387.

O'Sullivan, D.J. and Hitchman, M.H. (1992). Inertial instability and Rossby wave breaking in a numerical model. *J. Atmos. Sci*., 49, 991–1002, doi: 10.1175/1520-0469.

O'Sullivan D.J. and Salby, M.L. (1990). Coupling of the quasi-biennial oscillation and the extratropical circulation in the stratosphere through planetary wave transport. *J. Atmos. Sci.* 47, 650–673.

O'Sullivan, D.J. and Young, R.E. (1992). Modeling the quasi-biennial oscillation's effect on the winter stratospheric circulation. *J. Atmos. Sci*., 49, 2437–2448, doi:10.1175/1520-0469.

Pascoe, C.L., Gray, L.J. and Scaife, A.A. (2006). A GCM study of the influence of equatorial winds on the timing of sudden stratospheric warmings. *Geophys. Res. Lett*.,33, L06825.

Peings, Y., Douville, H., Colin, J., Martin, D.S., & Magnusdottir, G. (2017). Snow-NAO teleconnection and its modulation by the Quasi-Biennial Oscillation. *J. Clim.*, 30, 10,211–10,235.

Plumb, R.A. and Bell, R.C. (1982). A model of the quasi-biennial oscillation on an equatorial beta-plane. *Quart. J. Roy. Meteor. Soc.*, 108, 335-352, doi:10.1002/qj.49710845604.

Polvani, L.M. and Saravanan, R.R. (2000). The three-dimensional structure of breaking Rossby waves in the polar wintertime stratosphere. *J. Atmos. Sci.,* 57, 3663–3685.

Robock, A. (2000). Volcanic eruptions and climate. *Rev. Geophys.*, 38, 191– 219.

Ruzmaikin, A., Feynman, J., Jiang, X. and Yung, Y.L. (2005). Extratropical signature of the quasi-biennial oscillation. *J. Geophys. Res.*, 110, D11111.

Saha, S. *et al.* (2012). *NCEP Climate Forecast System Version 2 (CFSv2). Daily Products*. Research Data Archive at the National Center for Atmospheric Research, Computational and Information Systems Laboratory. https://doi.org/10.5065/D69021ZF. Accessed 10/07/2017.

Scaife, A.A., Athanassiadou, M., Andrews, M., Arribas, A., Baldwin, M., Dunstone, N., Knight, J., MacLachlan, C., Manzini, E., Müller, W.A., Pohlmann, H., Smith, D., Stockdale, T., and Williams, A. (2014). Predictability of the quasi-biennial oscillation and its northern winter teleconnection on seasonal to decadal timescales, *Geophys. Res. Lett*., 41, 1752–1758.

Schenzinger, V., Osprey, S., Gray, L.J. and Butchart, N. (2017). Defining metrics of the Quasi-Biennial Oscillation in global climate models, *Geosci. Model Dev.,* 10, 2157-2168.

Scherhag, R. (1952). Die explosionsartige Stratosphärenerwärmung des Spätwinters 1951/1952. Deutscher Wetterdienst (US Zone) 6:51–63.

Schoeberl, M.R. and Smith, A.K. (1986). The integrated enstrophy budget of the winter stratosphere diagnosed from LIMS data. *J. Atmos. Sci.,* 43, 1074–1086.

Schoeberl, M.R., Lait, L.R., Newman, P.A. and Rosenfield, J.E. (1992). The structure of the polar vortex. *J. Geophys. Res*., 97(D8), 7859–7882.

Scott, R.K. (2019). Nonlinear latitudinal transfer of wave activity in the winter stratosphere. *Q J R Meteorol Soc*., 1 - 14 doi.org/10.1002/qj.3536.

Scott, R.K and Dritschel, D.G. (2005). Quasi-geostrophic vortices in compressible atmospheres. *J. Fluid Mech*., 530, 305-325.

Simmons, A.J. and Hoskins, B.J. (1978). The life cycles of some nonlinear baroclinic waves. *J. Atmos. Sci.*, 35, 414-432.

Smith, A.K., Garcia, R.R., Moss, A.C. and Mitchell, N.J. (2017). The semiannual oscillation of the tropical zonal wind in the middle atmosphere derived from satellite geopotential height retrievals. *J. Atmos. Sci.,* 74, 2413–2425.

Tung, K.K. (1979). A theory of stationary long waves. Part III: Quasi-normal modes in a singular waveguide. *Mon. Wea. Rev*., 107, 751–774.

Tung, K.K. (1986). Nongeostrophic theory of zonally averaged circulation. Part I: Formulation. *J. Atmos. Sci*., 43, 2600–2618.

Waugh, D.W. and Dritschel, D.G. (1999). The Dependence of Rossby wave breaking on the vertical structure of the polar vortex. *J. Atmos. Sci.,* 56, 2359–2375.

Watson, P.A. G. and Gray, L.J. (2014). How does the quasi-biennial oscillation affect the stratospheric polar vortex? *J. Atmos. Sci.*, 71, 391-409.

White, I.P., Lu, H., Mitchell, N.J. and Phillips, T. (2015). Dynamical response to the QBO in the Northern Winter stratosphere: Signatures in wave forcing and eddy fluxes of potential vorticity. *J. Atmos. Sci*., 72, 4487–4507.

White, I.P., Lu, H. and Mitchell, N.J. (2016). Seasonal evolution of the QBO-induced wave forcing and circulation anomalies in the northern winter stratosphere. *J. Geophys. Res.*, 121, 10,411–10,431.

Yamashita, Y., Akiyoshi, H. and Takahashi, M. (2011). Dynamical response in the Northern Hemisphere midlatitude and high-latitude winter to the QBO simulated by CCSR/NIES CCM. *J. Geophys. Res.*, 116, D06118.

Zhang, J., Xie, F., Ma, Z., Zhang, C., Xu, M., Wang, T., and Zhang, R. (2019). Seasonal evolution of the quasi-biennial oscillation impact on the Northern Hemisphere polar vortex in winter.*J. Geophys. Res.*, 124, 12,568–12,586.

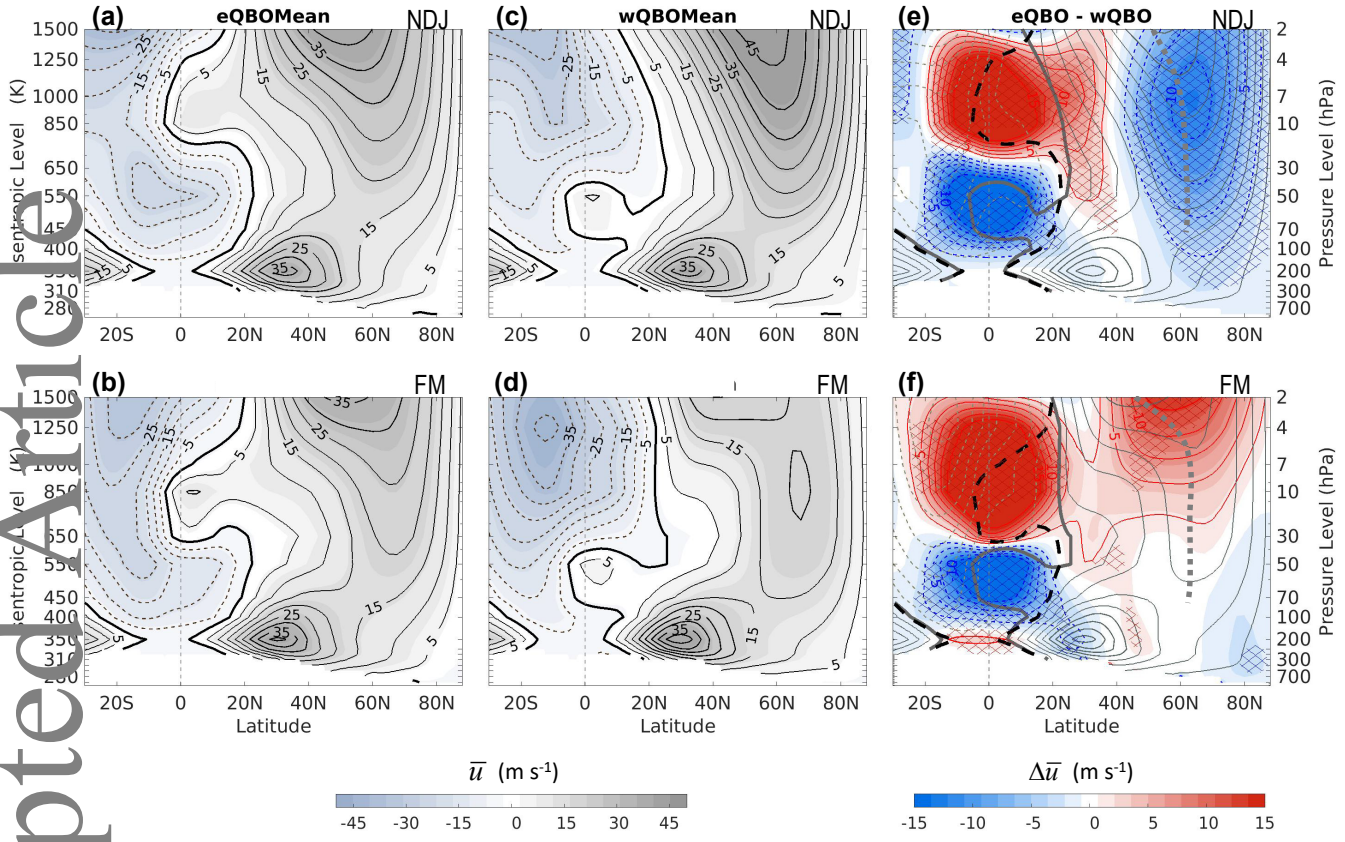

Fig. 1. (a, b): Zonal-mean zonal wind $\overline{u}$ during Nov-Jan and Feb-Mar for eQBO winter averages. Solid and dashed contours represent positive and negative winds with a contour interval of 5 m s^{1}. The zero-wind line is marked by the thick-black line. (c, d): same as (a, b) except for wQBO winters. (e, f): corresponding QBO composite differences (eQBO–wQBO) with red and blue shadings representing westerly and easterly anomalies. The colored contours have an interval of 2.5 m s^{-1}. The thick solid and dashed lines near the equator indicate the zero-wind lines for wQBO and eQBO, respectively. The average location of polar-vortex edge is indicated by the dotted lines in (e, f). The cross-hatchings specify statistical significance at 95% levels.

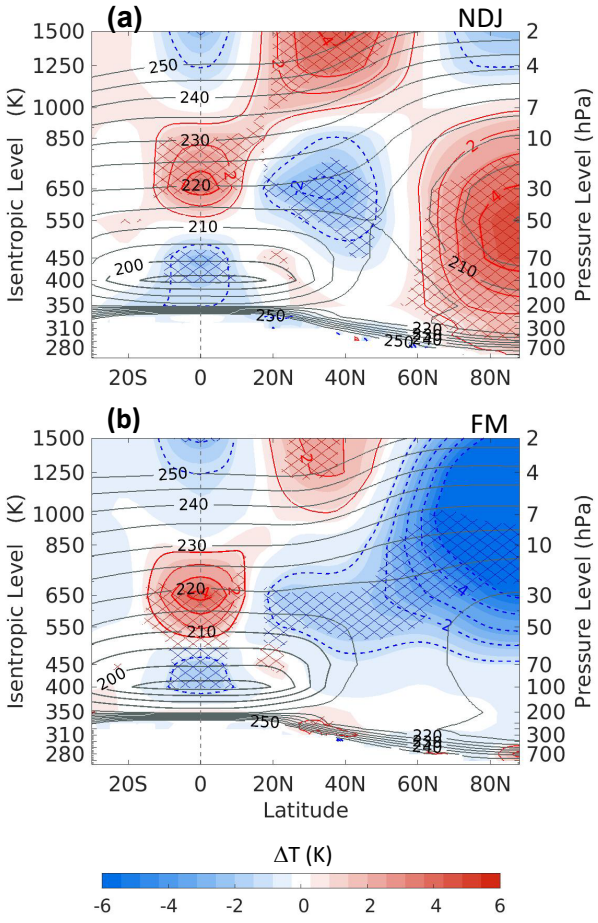

Fig. 2. Climatology (grey-lined contours with 5°K interval) and corresponding QBO composite differences (eQBO−wQBO) of the zonal-mean temperature $\overline{T}$ during Nov-Jan (a) and Feb-Mar (b), with 1°K interval.

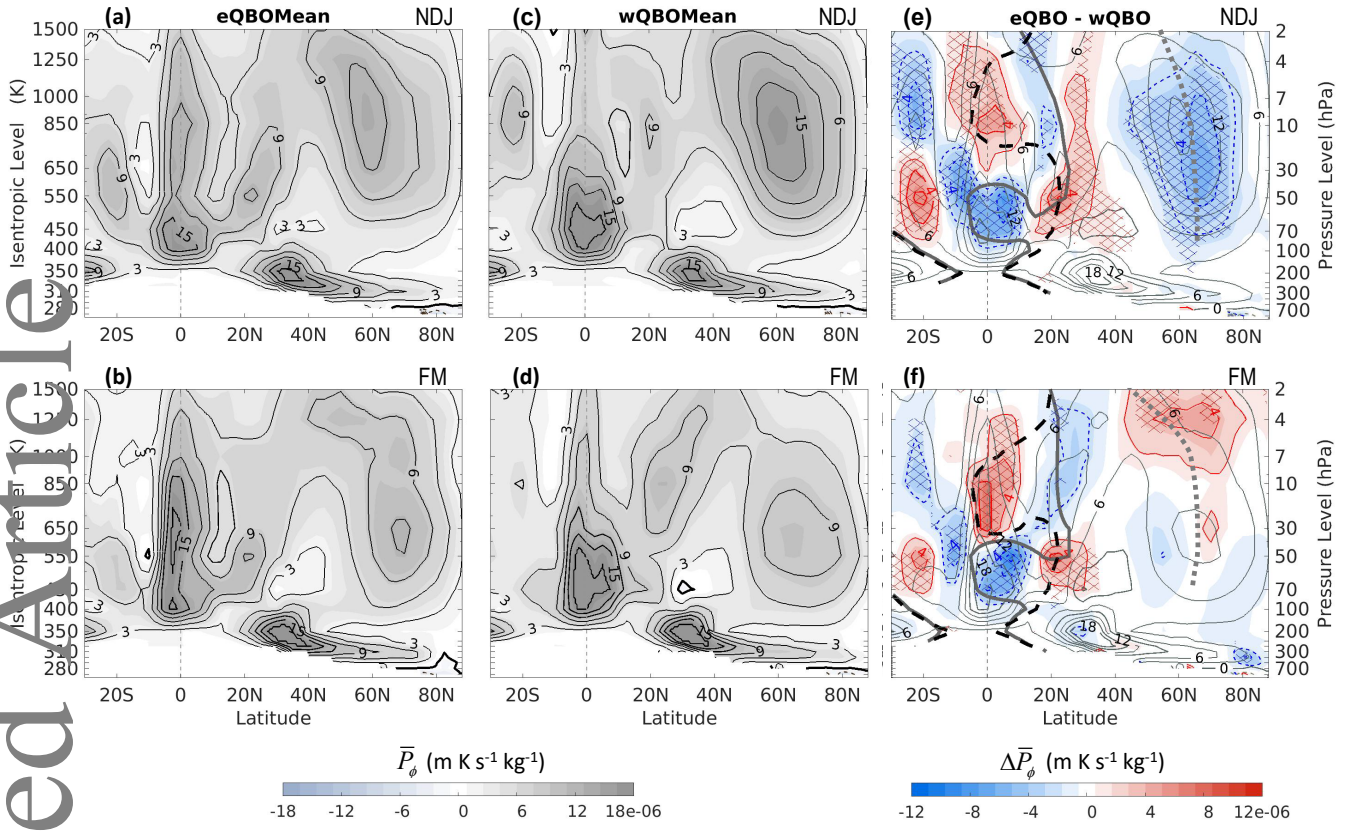

Fig. 3. (a-d): Same as Fig. 1(a-d) except for zonal-mean meridional PV gradient $\overline{P}_\phi$ with a contour interval of 2.5 × 10^{-6} K m kg^{-1} s^{-1}. Following Lait (1994), $\overline{P}_\phi$ is multiplied by $(\theta/350)^{-9/2}$ to account for its exponential increase with height. (e,f): corresponding QBO composite difference (eQBO–wQBO) of $\overline{P}_\phi$ (color shaded) with climatological $\overline{P}_\phi$ (grey contours) with a contour interval of 2 × 10^{-6} K m kg^{-1} s^{-1}. The eQBO and wQBO zero-wind lines (i.e. thick solid and dashed lines near the equator) and the average location of polar-vortex edge (grey dotted line) are shown. The cross-hatchings indicate statistical significance at 95% levels.

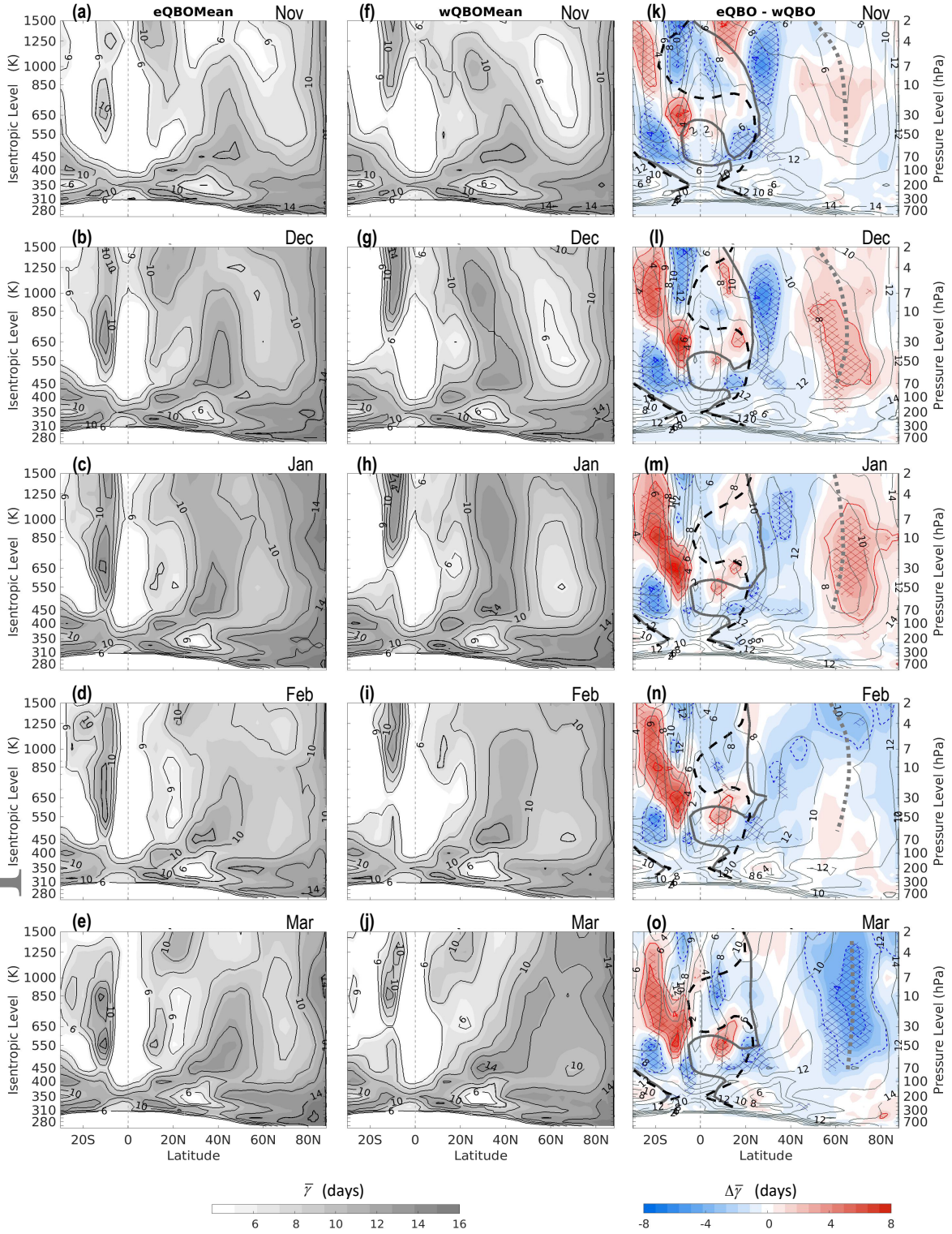

Fig. 4. (a-e): seasonal march (November to March) of the frequency of daily reversal of meridional PV gradients $\overline{\gamma}$ (in days per month) for eQBO winter mean. The contour interval is 2-day. (f-j): same as (a-e) except for wQBO mean. Regions with large values of $\overline{\gamma}$ are shaded in dark-grey to highlight the surf zone. (k-o): corresponding QBO composite differences (eQBO–wQBO) of $\overline{\gamma}$ (color shaded) with climatology (grey contours) with a contour interval of 2-day. QBO zero-wind lines (solid and dashed lines) and the average location of polar-vortex edge (dotted lines) are added for location references.

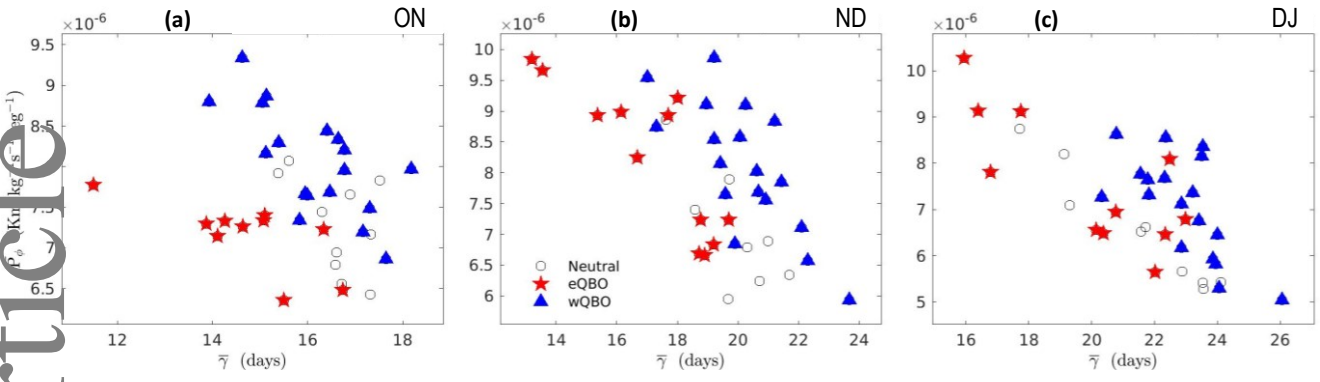

Fig. 5. (a): scatter plots between the Oct-Nov averaged zonal-mean frequency of daily reversal of meridional PV gradients $\bar{\gamma}$ and the corresponding meridional PV gradient $\bar{P}_\phi$ at 20-45°N, 850-1250 K, where the surf zone is formed climatologically. Red stars and blue triangles indicate eQBO and wQBO winters while open grey circles indicate neutral winters. (b, c): same as (a) except for Nov-Dec and Dec-Jan averages. Note that $\bar{P}_\phi$ is scaled by $(\theta/350)^{-9/2}$.

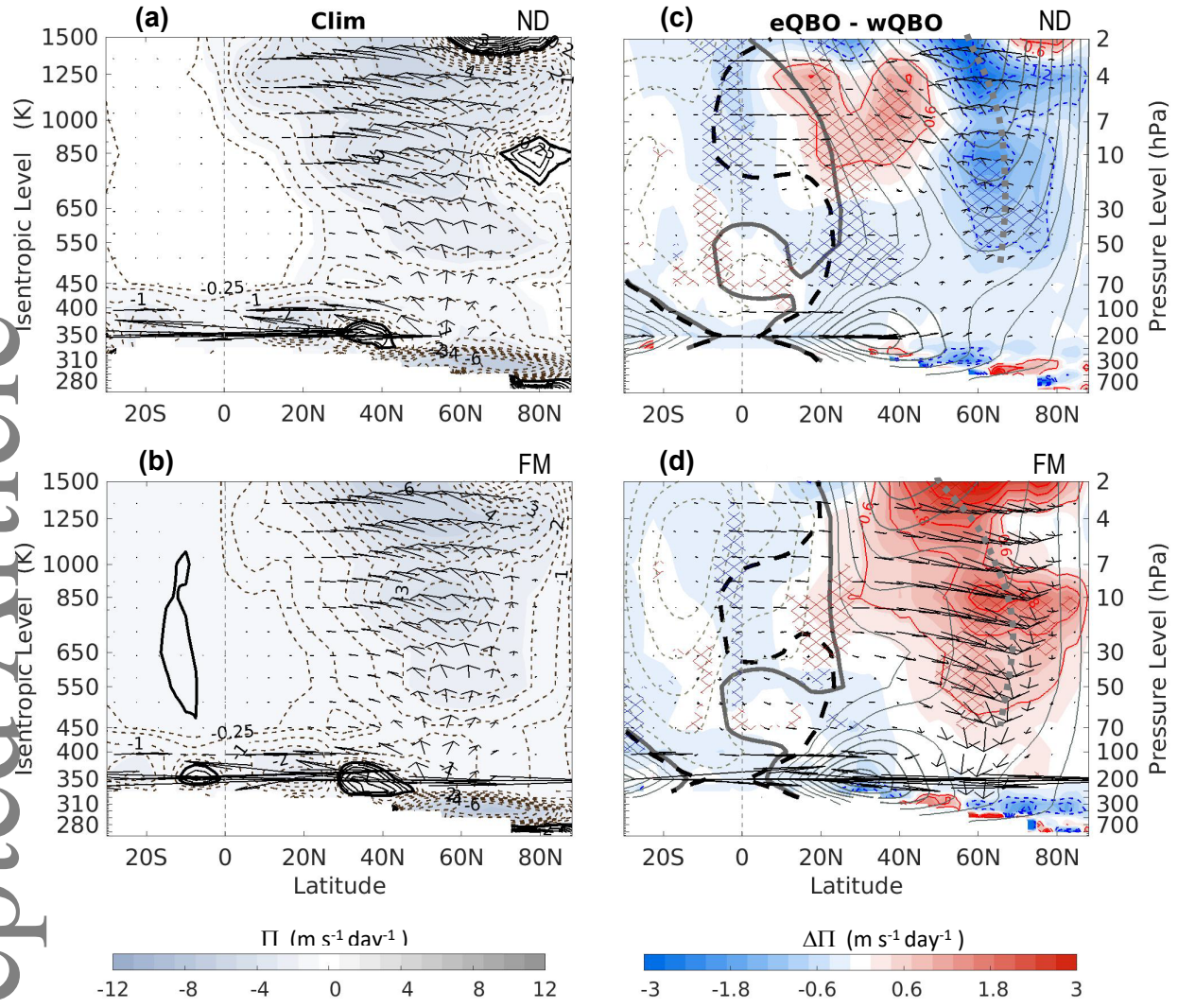

Fig. 6. (a, b): Climatology of the Nov-Dec and Feb-Mar averaged EP fluxes (arrows) and the eddy PV fluxes Π (contours at ±0.25, 0.5, 1, 1.5 2, 2.5, 3, 3.5, 4, 5, 6, 7, 8, 10, 12 m s^{-1} day^{-1}). The EP fluxes have been scaled to account for their rapid decrease of magnitudes with height and to make the magnitudes of $F^{(\phi)}$ and $F^{(\theta)}$ comparable for better visualisation. All the contour lines, the thick solid and dotted lines are the same as Fig. 1. (c, d): corresponding QBO composite differences (eQBO–wQBO) with contour interval of 0.6 m s^{-1} day^{-1}. Climatological $\overline{u}$ (grey contours), QBO zero-wind lines (eQBO solid and wQBO dashed lines) and the average location of polar-vortex edge (grey dotted lines) are added for location references. The cross-hatchings indicate statistical significance at 95% levels.

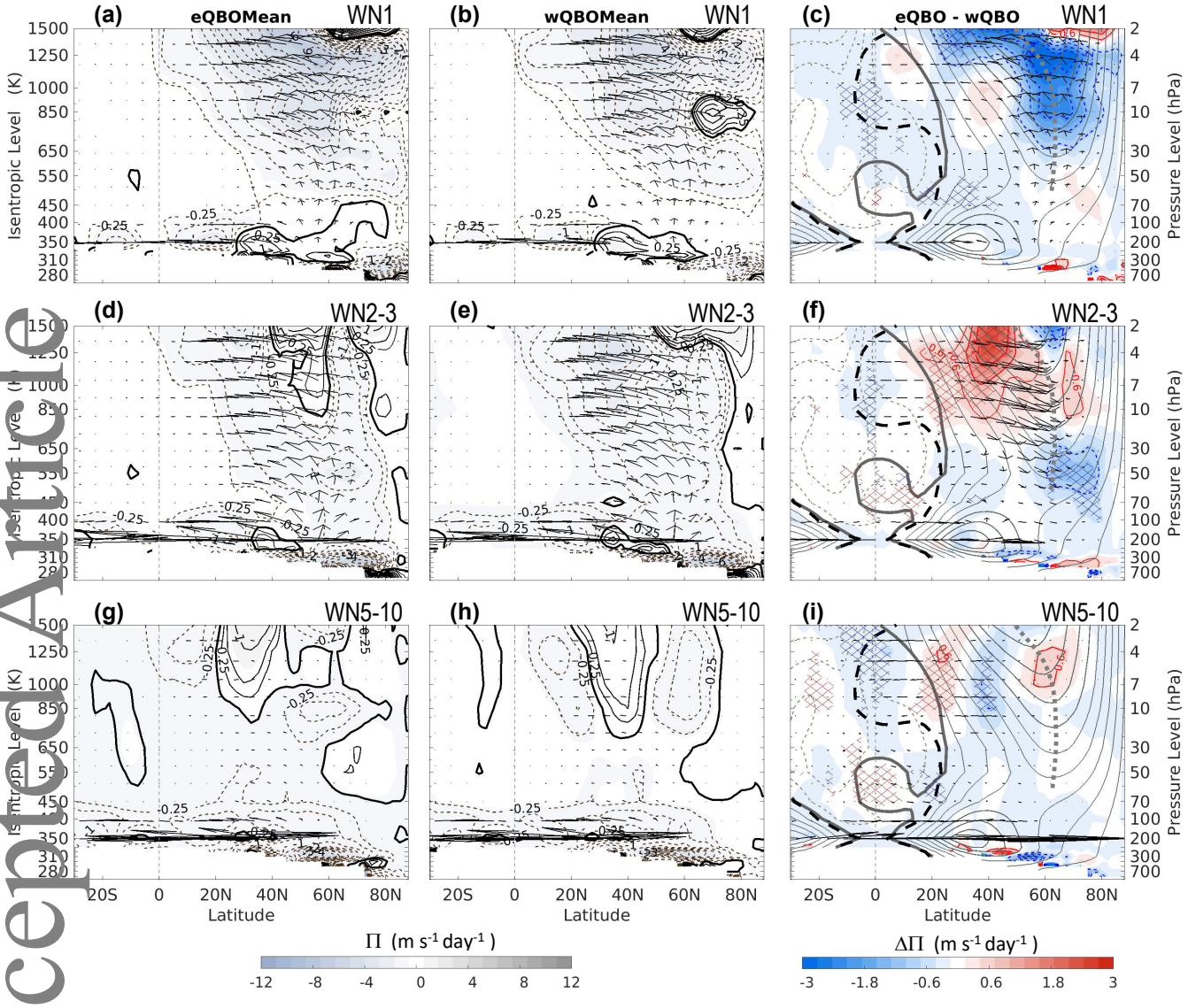

Fig. 7. (a-c): Nov-Dec averaged wave-1 EP fluxes (arrows) and the eddy PV fluxes Π (in m s^{-1} day^{-1}) (contours) for eQBO, wQBO and their differences (eQBO–wQBO). (d-f): same as (a-c) except wave-2-3. (g-i): same as (a-c) except wave-5-10. Other lines, contours and hatches are same as in fig. 6.

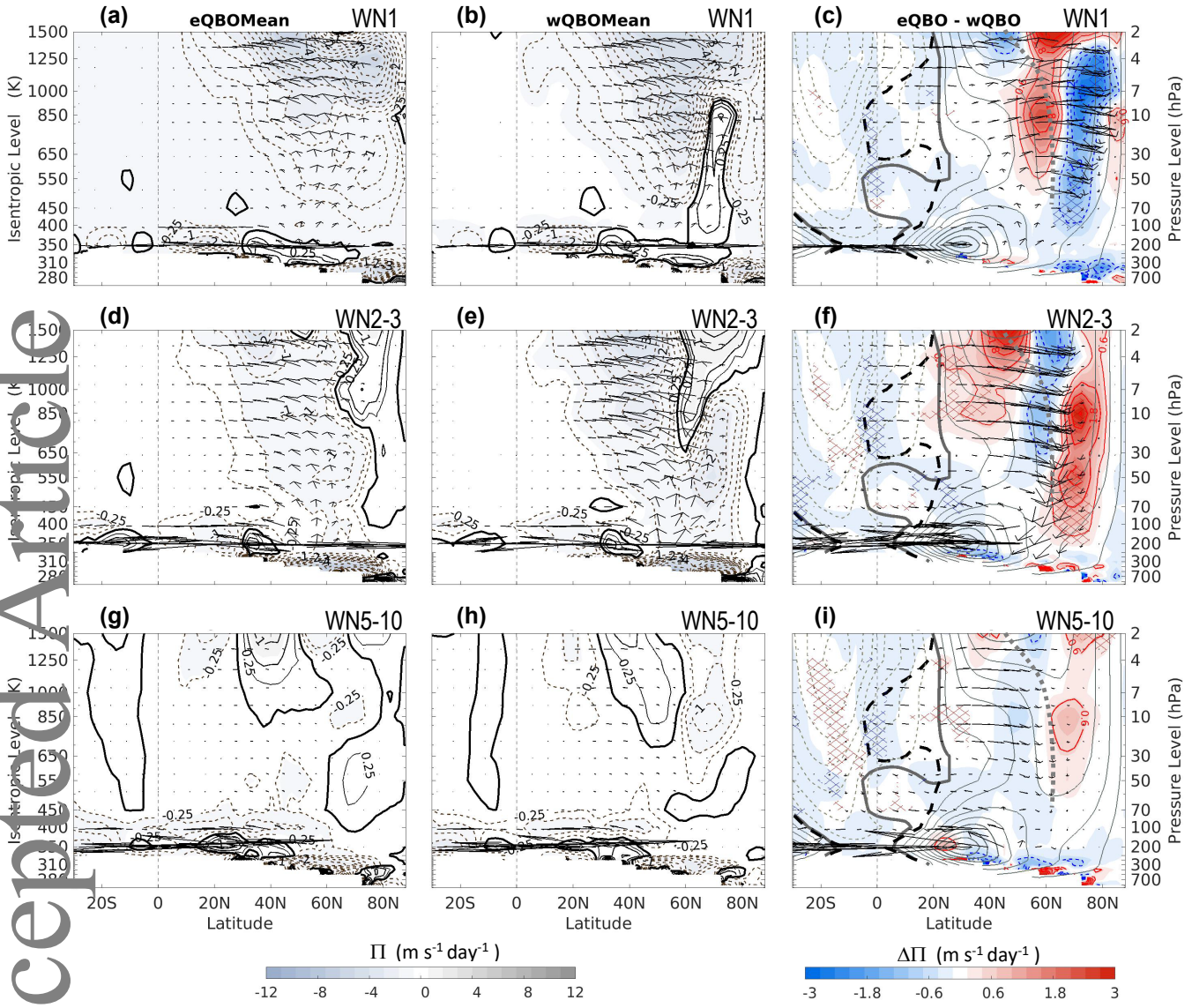

Fig. 8. Same as Fig. 7 except for Feb-Mar averages.

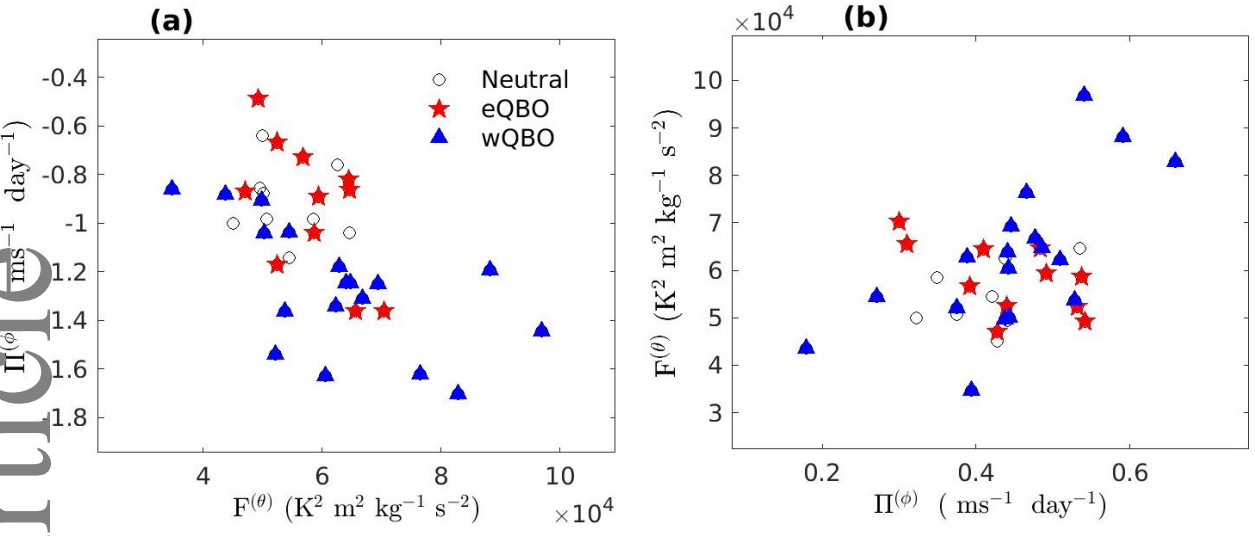

Fig. 9. (a): scatter plot between Jan-Mar mean vertical component of wave-2-3 EP fluxes $F^{(\theta)}$ at 35-70°N, 350-450 K and Jan-Mar mean meridional component of wave-2-3 EP-flux divergence Π_{ϕ} at 20-40°N, 1000-1500 K. (b): Dec-Feb mean meridional component of wave-2-3 EP-flux divergence Π_{ϕ} at 35-70°N, 350-650 K and Jan-Mar mean vertical component of wave-2-3 EP fluxes $F^{(\theta)}$ at 35-70°N, 350-450 K. Red stars and blue triangles indicate eQBO and wQBO winters while open grey circles indicate neutral winters.

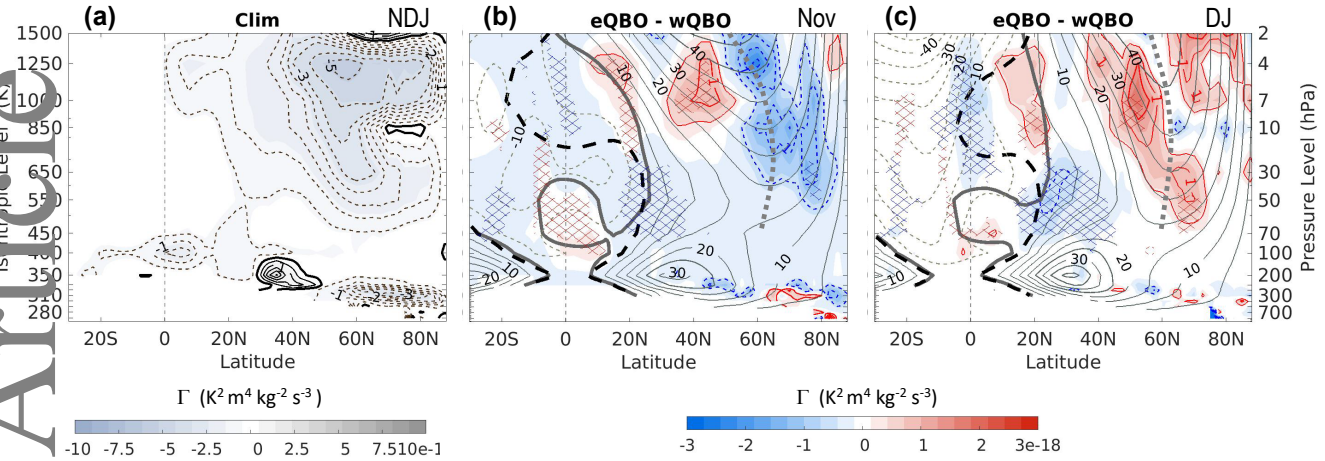

Fig. 10 (a): climatology of the Nov-Jan averaged down-gradient eddy PV flux Γ, which is scaled by multiplied it by $(\theta/350)^{-18/2}$ with contours at ±0.5, 1, 1.5 2, 2.5, 3, 4, 5, 6, 7, 8, 10, 12 × 10^{-18} $K^2\,m^4\,kg^{-2}\,s^{-3}$. (b, c): QBO composite differences (eQBO−wQBO) averaged for November and Dec-Jan with contour interval of ±0.5 × 10^{-18} $K^2\,m^4\,kg^{-2}\,s^{-3}$. Climatological $\overline{u}$ (grey contours), QBO zero-wind lines (solid and dashed lines) and the average location of polar-vortex edge (dotted lines) are added for location references.

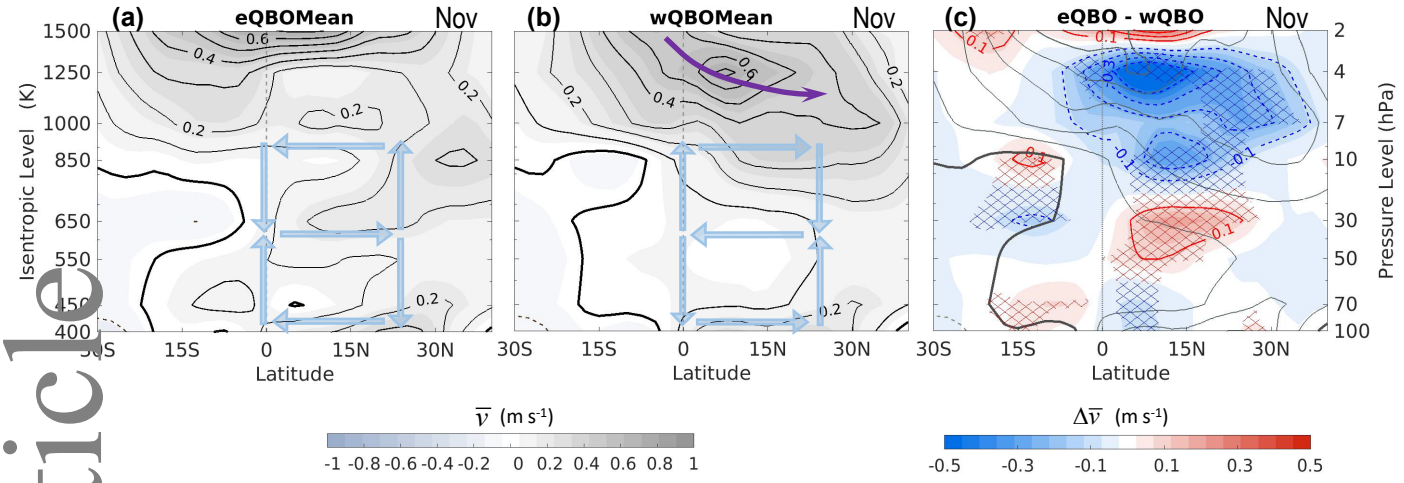

Fig. 11. (a, b): climatology of the November averaged zonal-mean meridional velocity $\overline{v}$ under eQBO and wQBO in the latitude region of 30°S-40°N with a contour interval of 0.1 m s^{-1}. The thick solid line indicates $\overline{v} = 0$. The blue arrows indicate the QBO-MMC. The purple semi-circle indicate westerly SAO that is typically enhanced under wQBO. (c): corresponding QBO composite differences (eQBO–wQBO) (colored contours with inteval of 0.1 m s^{-1}). Climatological $\overline{v}$ is plotted as grey contours. The cross-hatchings specify statistical significance at 95% levels.

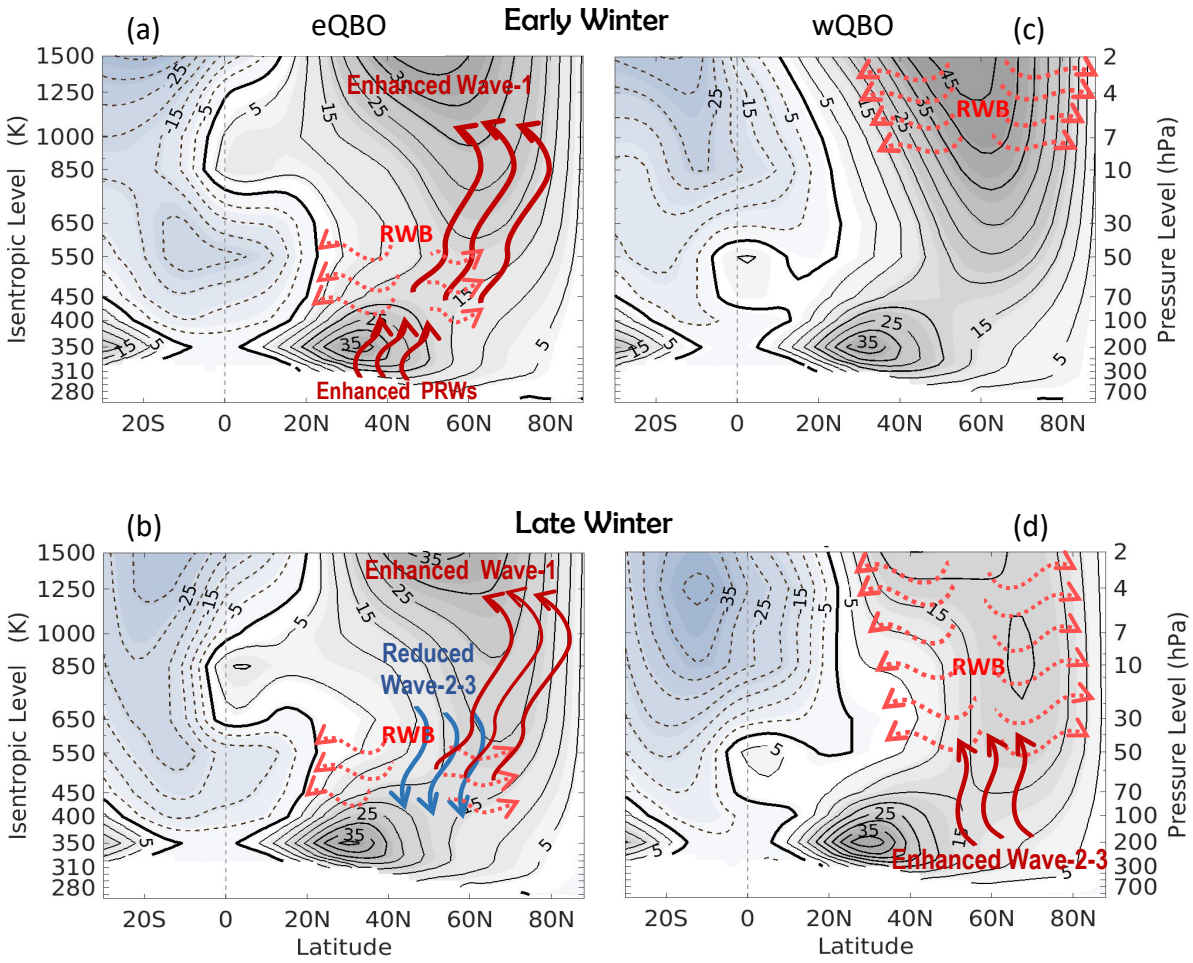

Fig. 12. Schematics of QBO modulation of vertically propagating PRWs and RWB during eQBO (a, b) and wQBO (c, d) and in early (a, c) and late (b, d) winters. The upward- (or downward-) pointing red (or blue) wiggling arrows indicate enhanced (or reduced) upward propagation of PRWs with relevant wavenumbers indicated by the text below or above. The meridional diverging dotted-wiggled arrows indicate RWB. The grey contours are seasonal averaged zonal-mean zonal winds. See text for detailed explanations.